TMEX 2023, Quy Nhon

Detection of the Sagittarius Dwarf Spheroidal Galaxy in Gamma-Rays

Roland Crocker

Australian National University

Gamma-Ray Emission from the Sagittarius Dwarf Spheroidal Galaxy due to Millisecond Pulsars,
Crocker, Macias et al., Nature Astr. (2022)
[arXiv:2204.12054]

Roland M. Crocker[1,10,*,+], Oscar Macias[2,3,†,+], Dougal Mackey[1], Mark R. Krumholz[1], Shin'ichiro Ando[2,3], Shunsaku Horiuchi[4,3], Matthew G. Baring[5], Chris Gordon[6], Thomas Venville[7], Alan R. Duffy[7], Rui-Zhi Yang[8,9,10], Felix Aharonian[10,11], J. A. Hinton[10], Deheng Song[4], Ashley J. Ruiter[12], and Miroslav D. Filipović[13]

Gamma-Ray Emission from the Sagittarius Dwarf Spheroidal Galaxy due to Millisecond Pulsars,
Crocker, Macias et al., Nature Astr. (2022)
[arXiv:2204.12054]

Roland M. Crocker[1,10,*,+], Oscar Macias[2,3,†,+], Dougal Mackey[1], Mark R. Krumholz[1], Shin'ichiro Ando[2,3], Shunsaku Horiuchi[4,3], Matthew G. Baring[5], Chris Gordon[6], Thomas Venville[7], Alan R. Duffy[7], Rui-Zhi Yang[8,9,10], Felix Aharonian[10,11], J. A. Hinton[10], Deheng Song[4], Ashley J. Ruiter[12], and Miroslav D. Filipović[13]

Gamma-Ray Emission from the Sagittarius Dwarf Spheroidal Galaxy due to Millisecond Pulsars,
Crocker, Macias et al., Nature Astr. (2022)
[arXiv:2204.12054]

Roland M. Crocker[1,10,*,+], Oscar Macias[2,3,†,+], Dougal Mackey[1], Mark R. Krumholz[1], Shin'ichiro Ando[2,3], Shunsaku Horiuchi[4,3], Matthew G. Baring[5], Chris Gordon[6], Thomas Venville[7], Alan R. Duffy[7], Rui-Zhi Yang[8,9,10], Felix Aharonian[10,11], J. A. Hinton[10], Deheng Song[4], Ashley J. Ruiter[12], and Miroslav D. Filipović[13]

Gamma-Ray Emission from the Sagittarius Dwarf Spheroidal Galaxy due to Millisecond Pulsars,
Crocker, Macias et al., Nature Astr. (2022)
[arXiv:2204.12054]

Roland M. Crocker[1,10,*,+], Oscar Macias[2,3,†,+], Dougal Mackey[1], Mark R. Krumholz[1], Shin'ichiro Ando[2,3], Shunsaku Horiuchi[4,3], Matthew G. Baring[5], Chris Gordon[6], Thomas Venville[7], Alan R. Duffy[7], Rui-Zhi Yang[8,9,10], Felix Aharonian[10,11], J. A. Hinton[10], Deheng Song[4], Ashley J. Ruiter[12], and Miroslav D. Filipović[13]

Fermi Bubbles substructure (?)

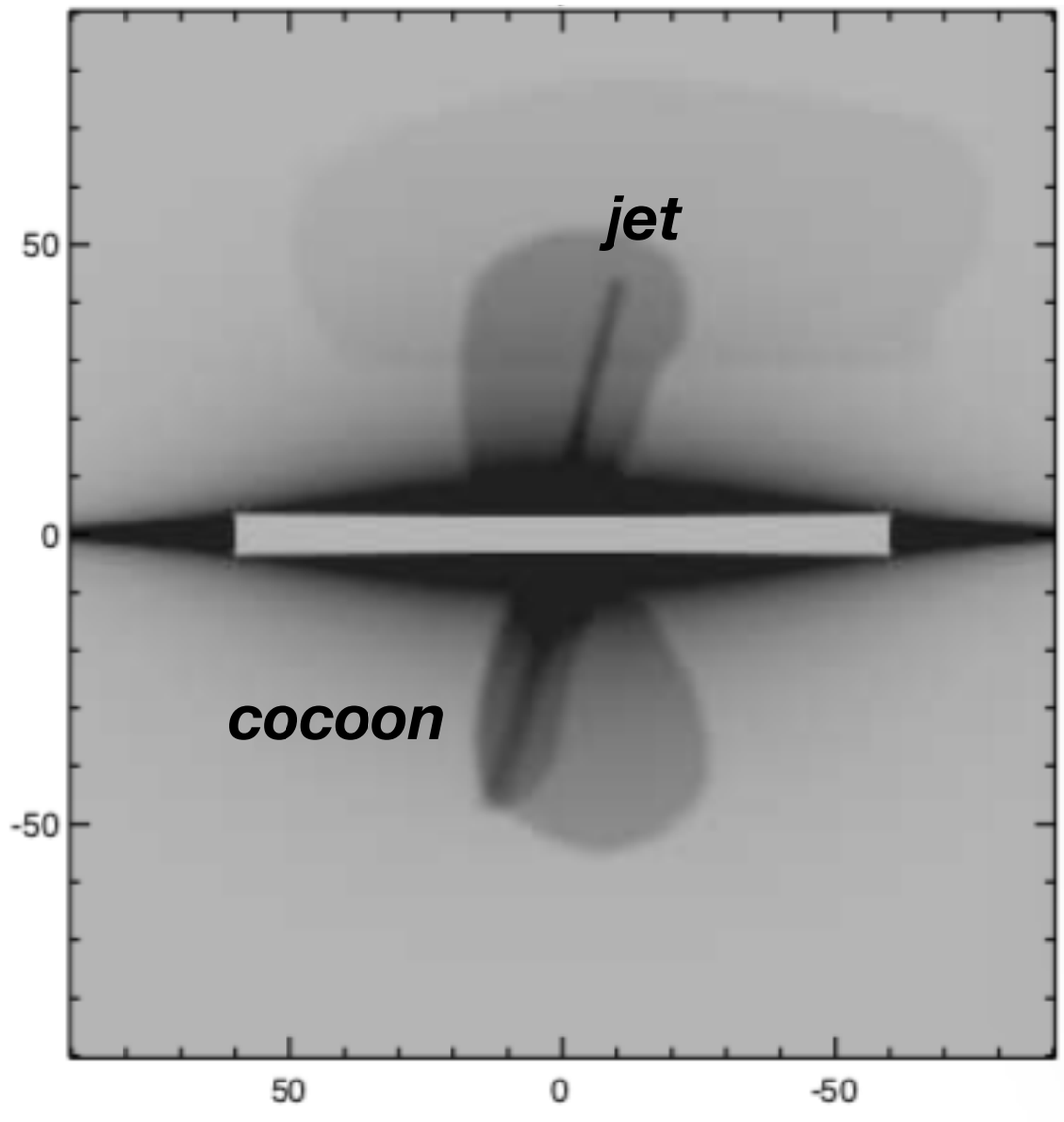

Su and Finkbeiner 2012

Fermi Bubbles substructure (?)

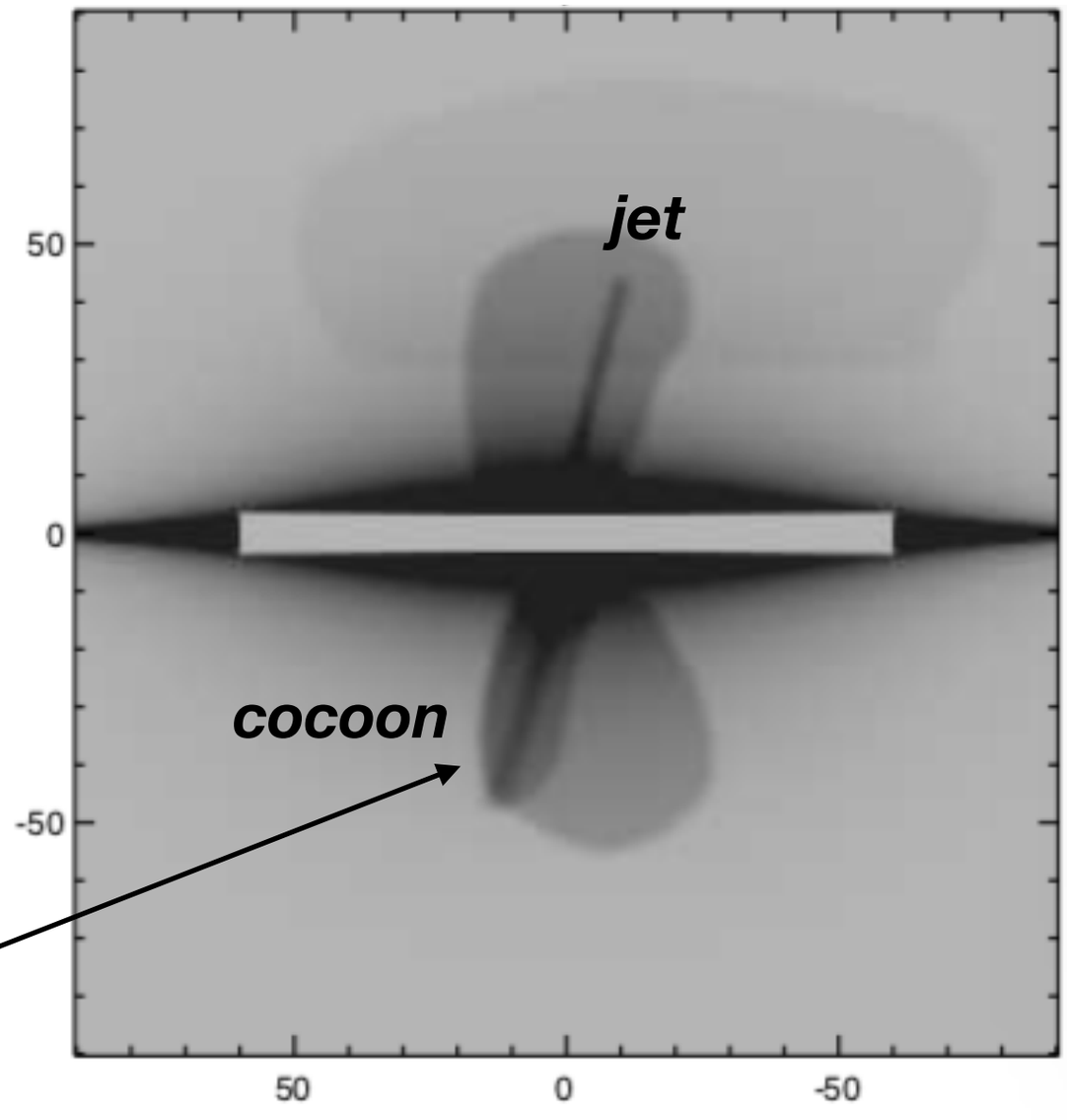

Templates developed for *Fermi* ~GeV γ-ray analysis

Su and Finkbeiner 2012

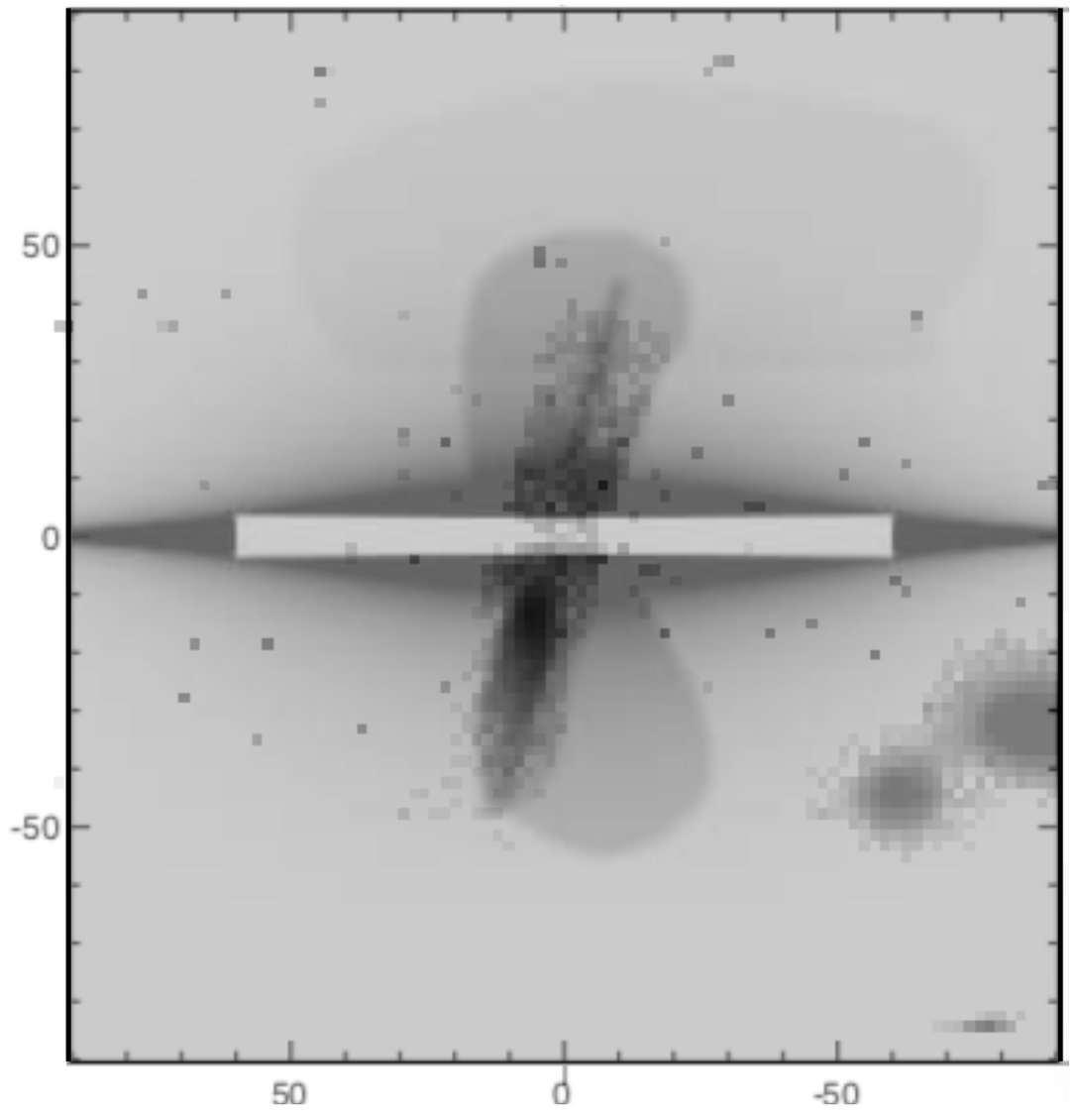
50
0
-50
50
0
-50

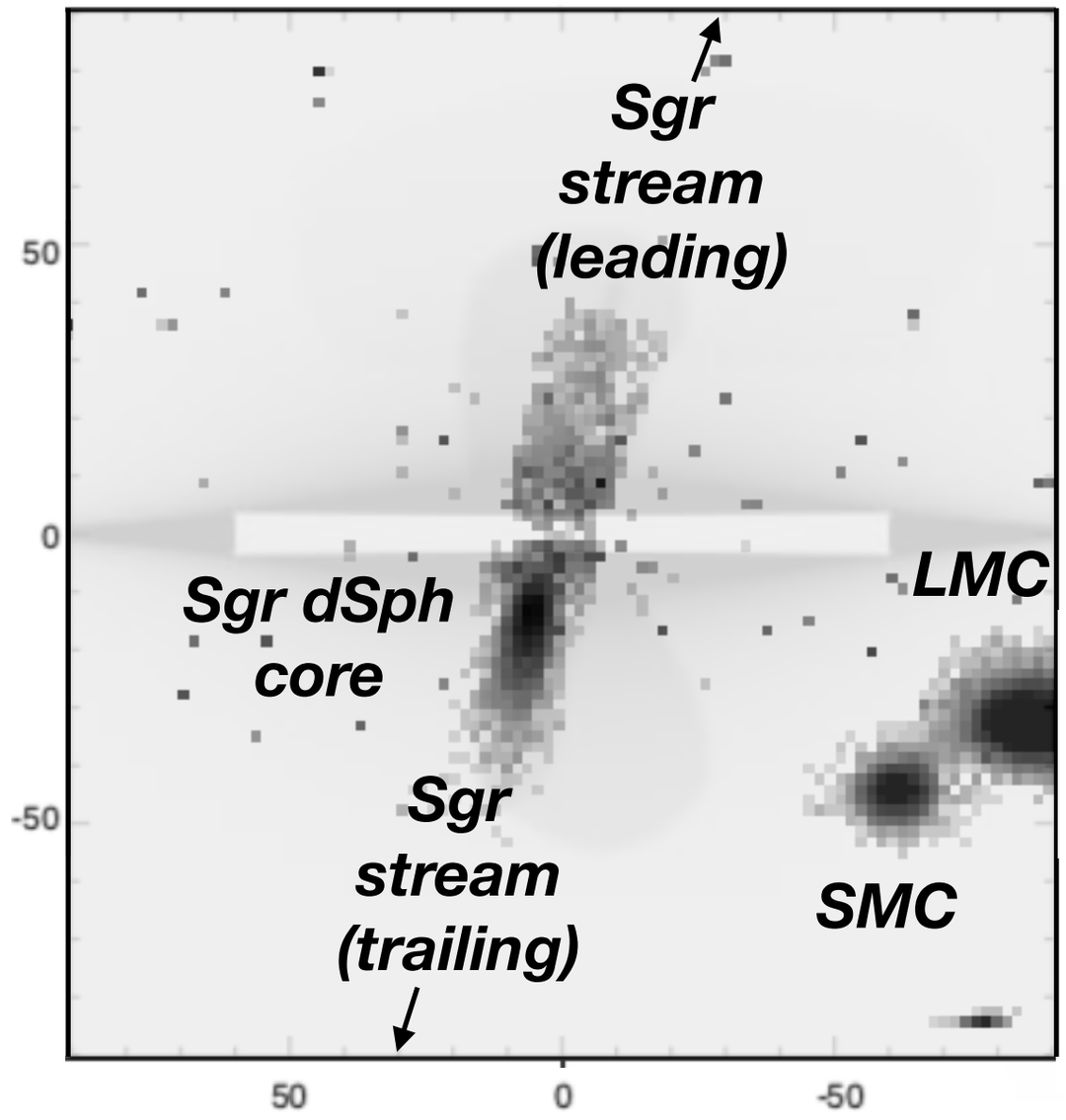

Iorio and Belokurov 2018

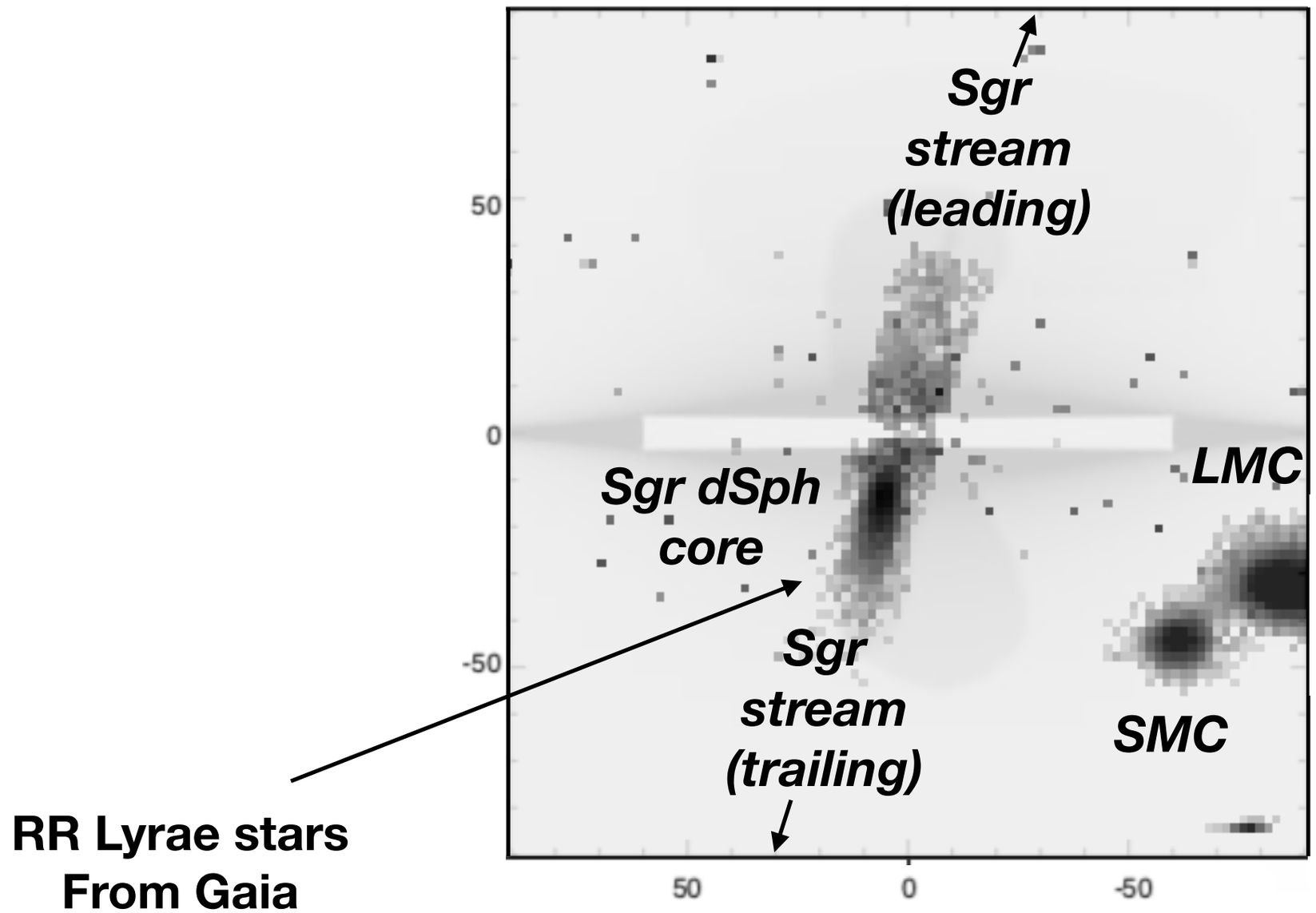

Iorio and Belokurov 2018

Sgr dSph and Fermi Bubbles ‘Cocoon’

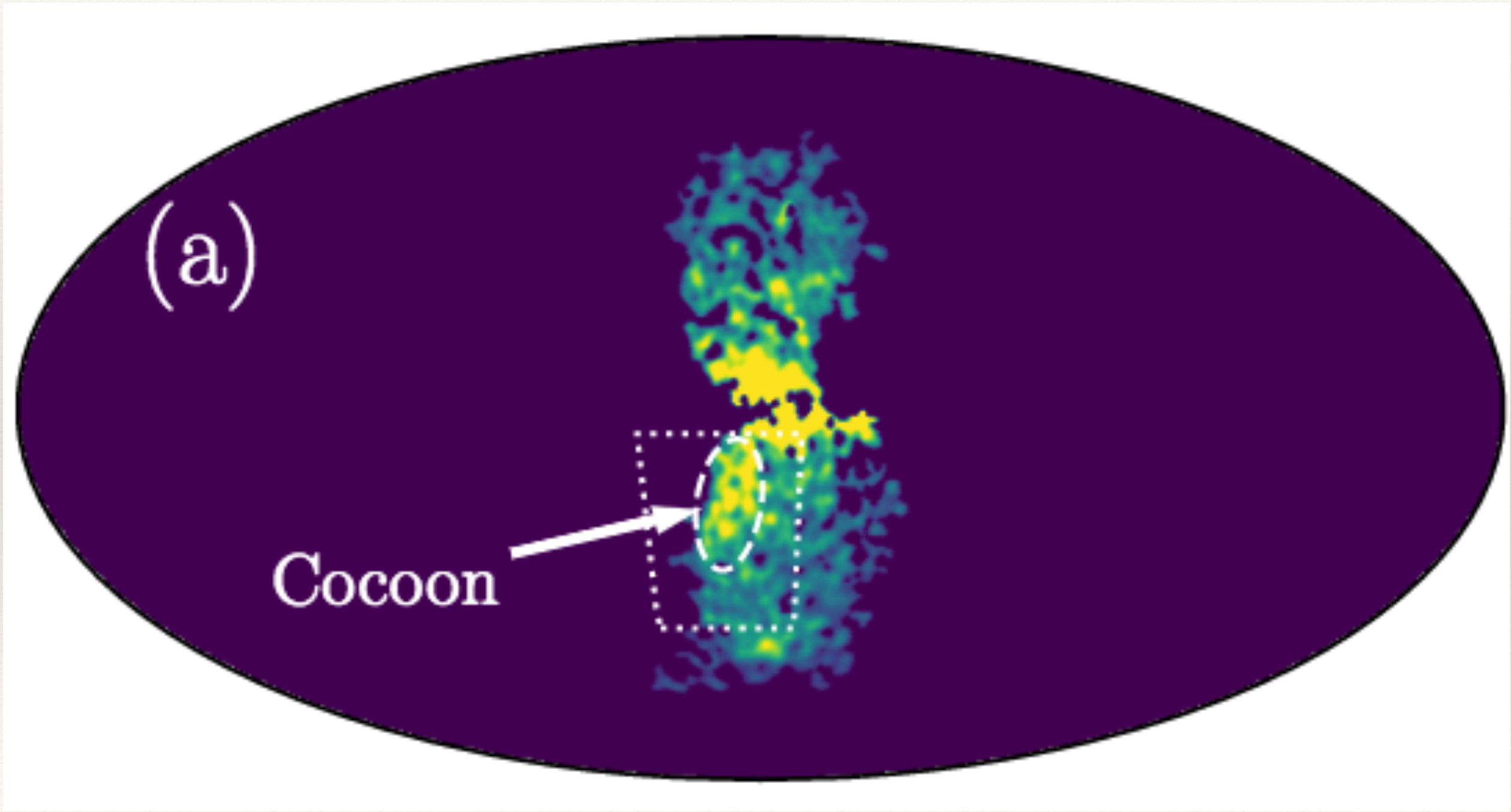

Fermi Bubbles **template defined by the** ***Fermi*** **Collaboration**

Sgr dSph and Fermi Bubbles ‘Cocoon’

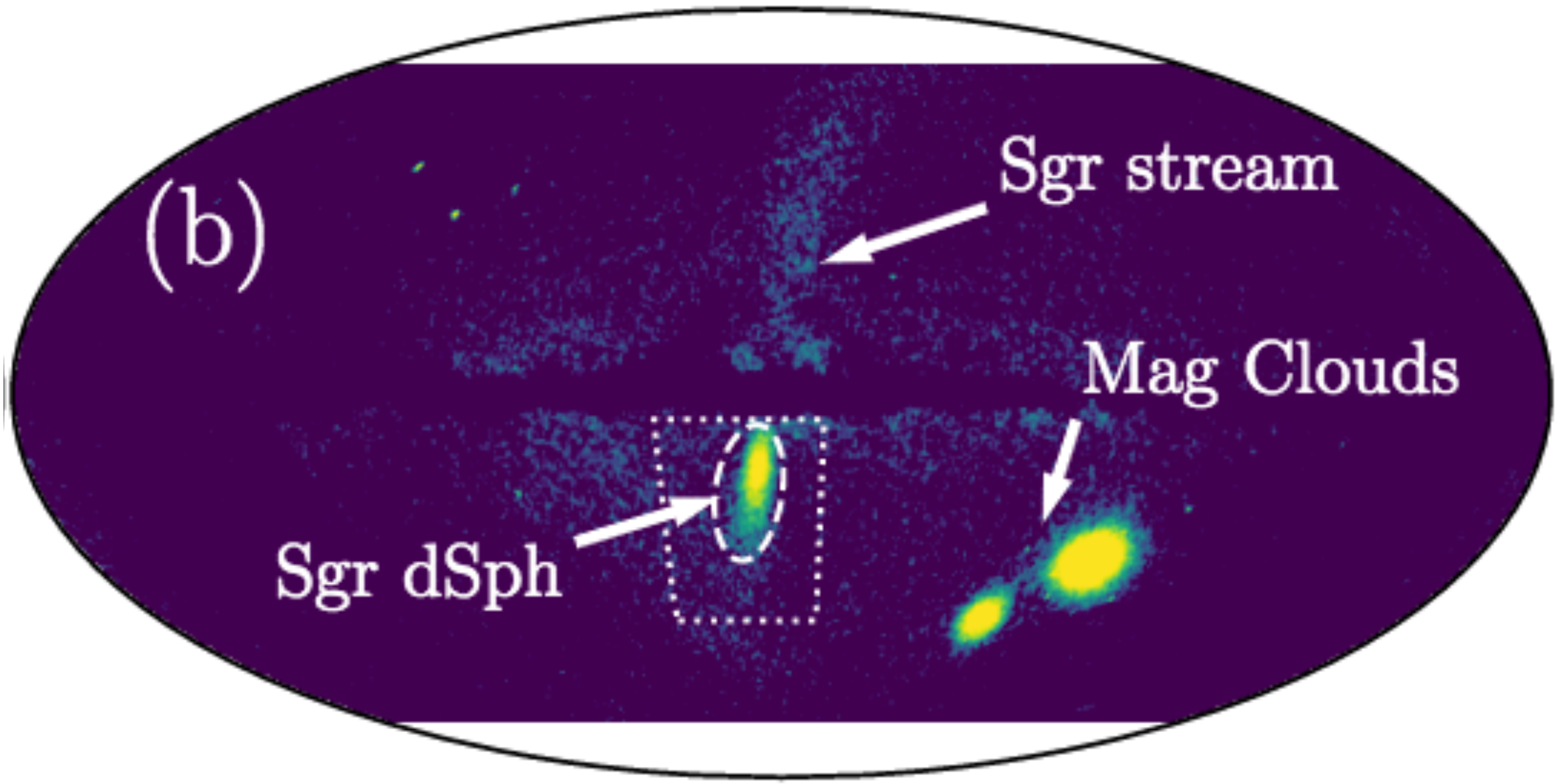

Gamma rays

RR Lyrae Stars

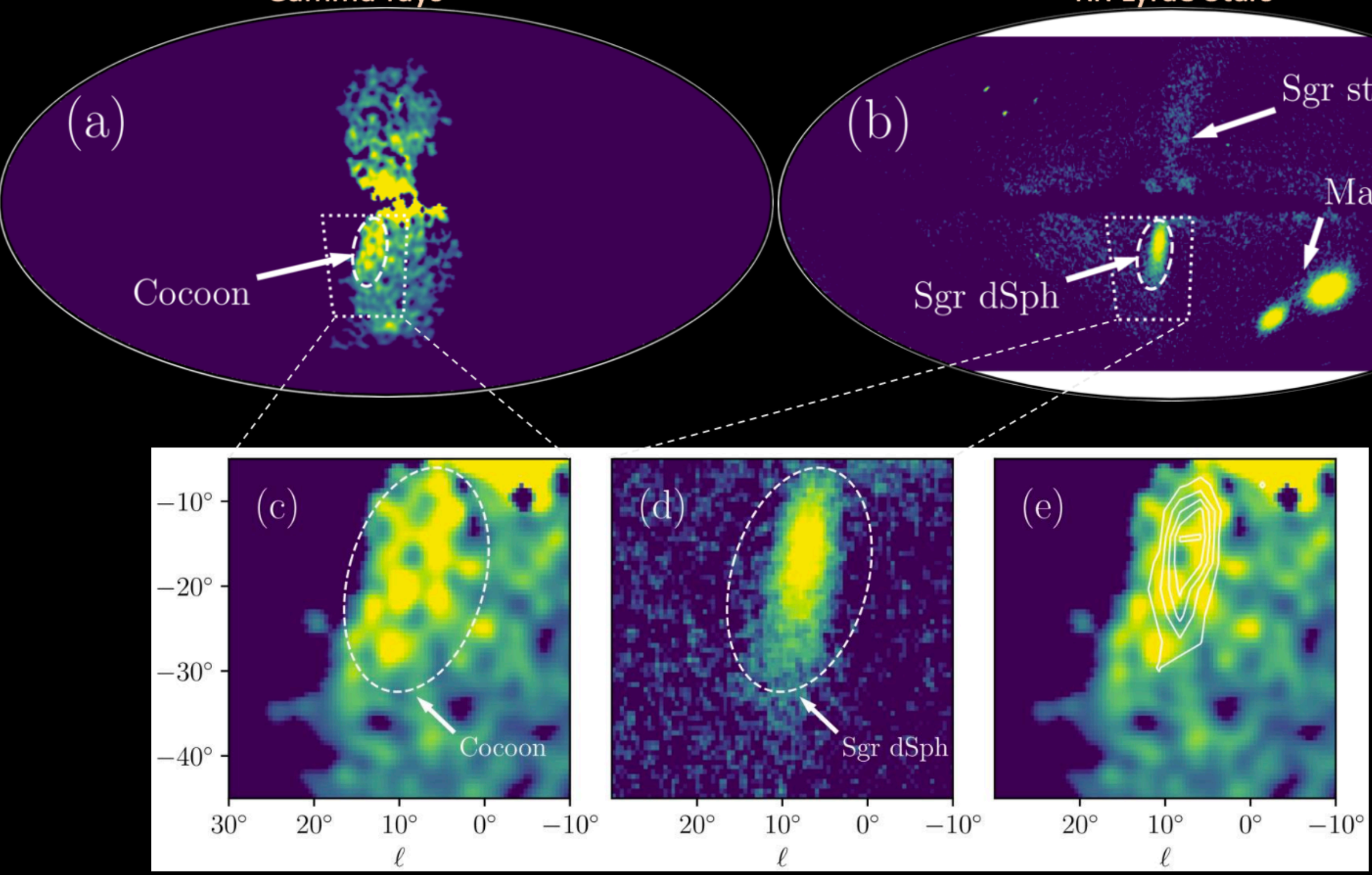

Gamma rays

RR Lyrae Stars

Context

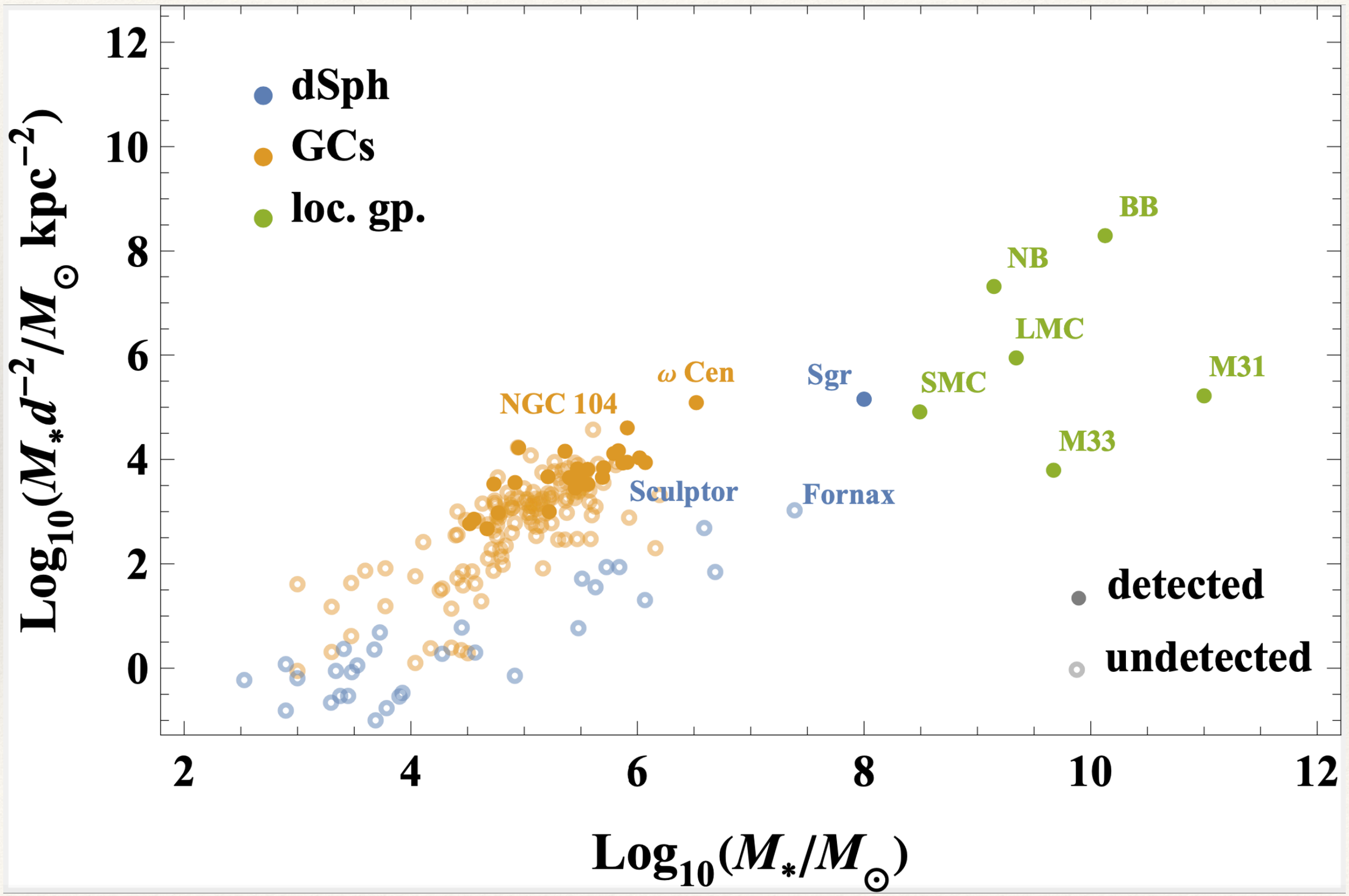
dSph
GCs
loc. gp.
BB
NB
LMC
M31
SMC
Sgr
ω Cen
NGC 104
M33
Sculptor
Fornax
detected
undetected
12
10
8
6
4
2
0
2
4
6
8
10
12
Log10(M*d−2/M⊙ kpc−2)
Log10(M*/M⊙)

Context

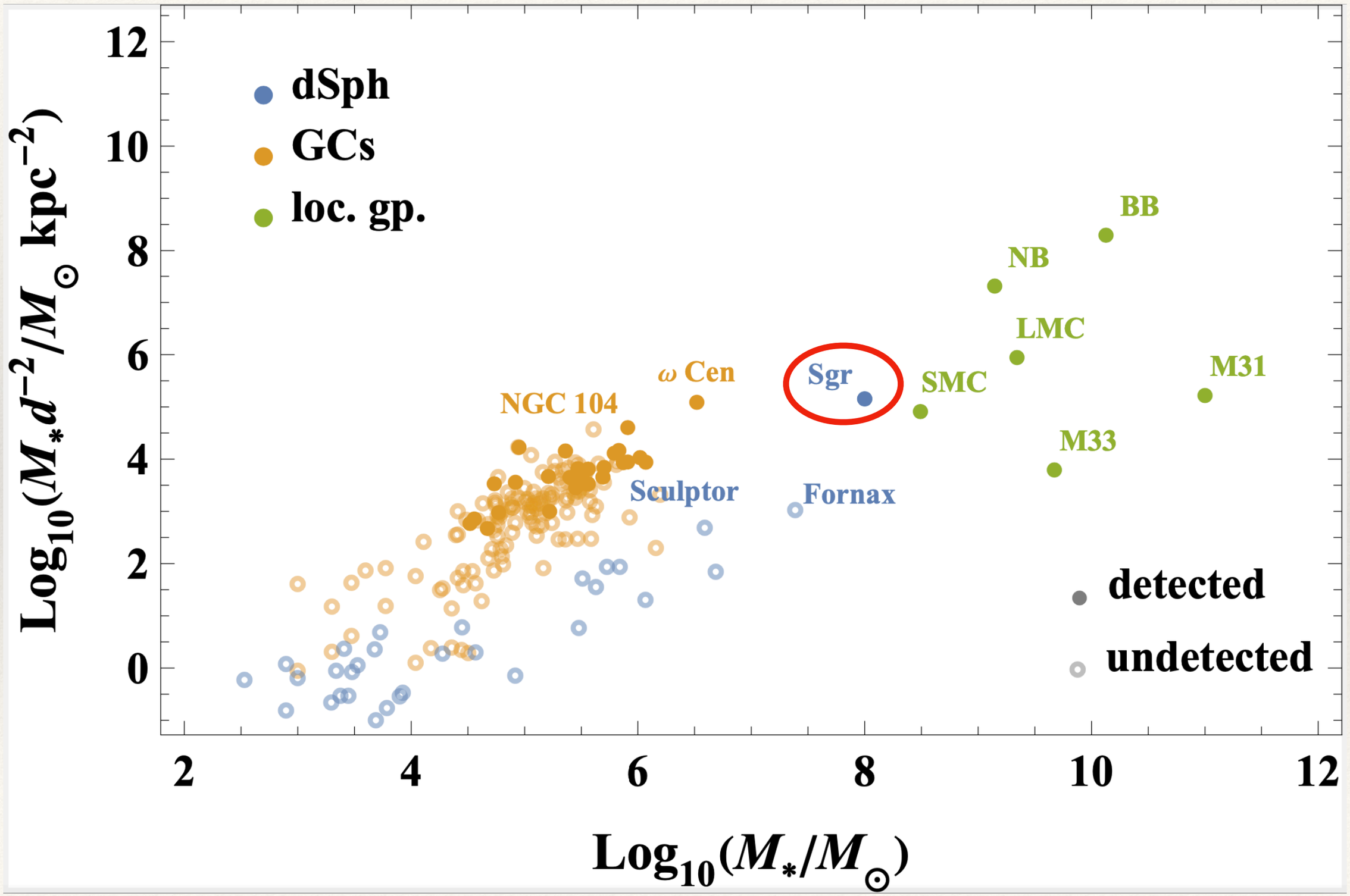
dSph
GCs
loc. gp.
BB
NB
LMC
M31
SMC
Sgr
ω Cen
NGC 104
M33
Sculptor
Fornax
detected
undetected
12
10
8
6
4
2
0
2
4
6
8
10
12
$\mathrm{Log}_{10}(M_*d^{-2}/M_\odot\ \mathrm{kpc}^{-2})$
$\mathrm{Log}_{10}(M_*/M_\odot)$

Aya Tsuboi, Kavli IPMU

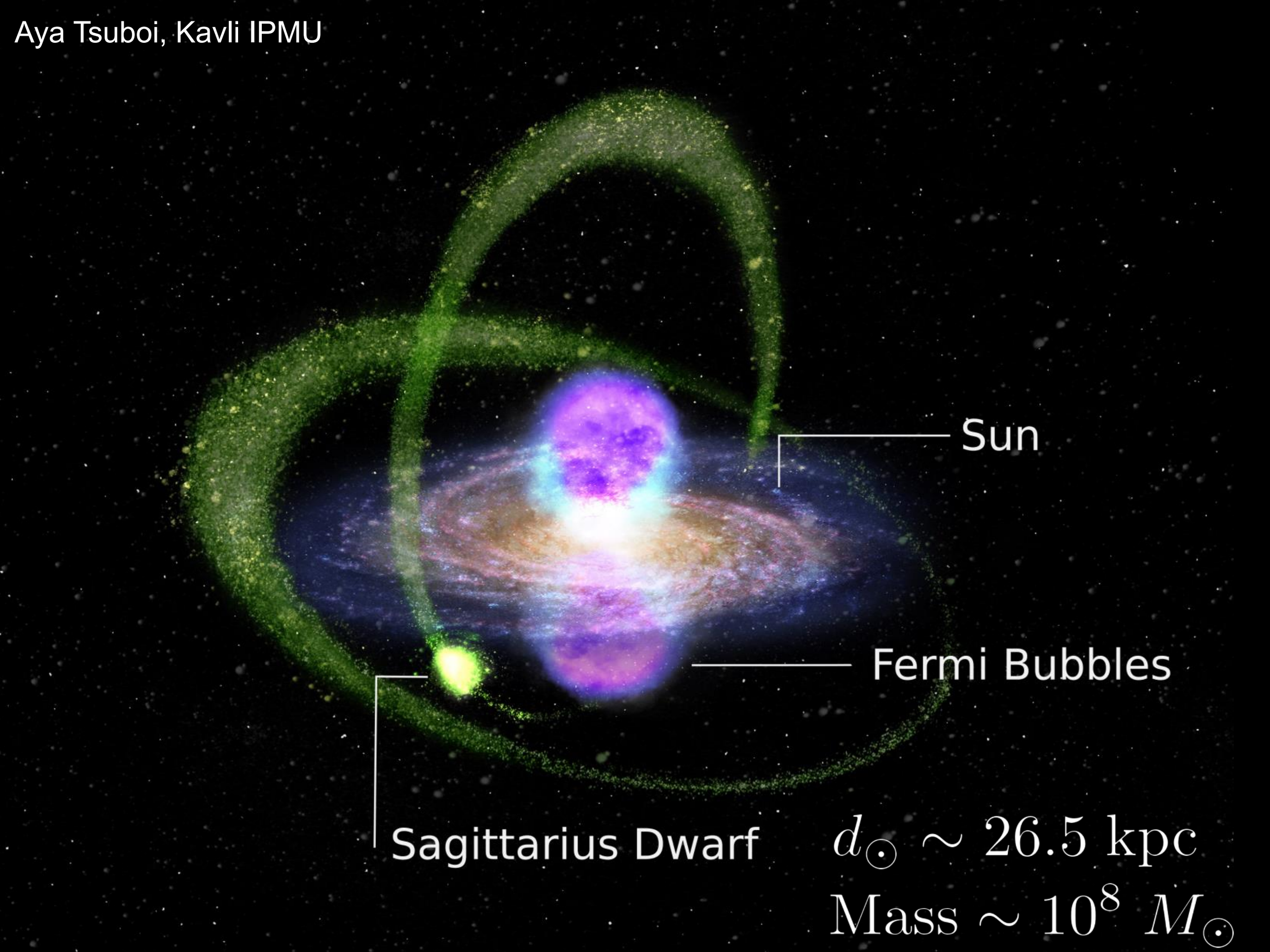

Detection significance

Template choices				Results			
Hadr. / Bremss.	IC	FB	Sgr dSph	$-\log(\mathscr{L}_{\text{Base}})$	$-\log(\mathscr{L}_{\text{Base+Sgr}})$	$\text{TS}_{\text{Source}}$	Significance
				Default model			
HD	3D	S	Model I	866680.6	866633.0	95.2	8.1 σ
				Alternative background templates			
HD	2D A	S	Model I	866847.1	866810.9	72.3	6.9 σ
HD	2D B	S	Model I	867234.9	867192.1	85.8	7.8 σ
HD	2D C	S	Model I	866909.4	866868.5	81.7	7.4 σ
Interpolated	3D	S	Model I	867595.4	867567.4	56.0	5.8 σ
GALPROP	3D	S	Model I	866690.5	866640.8	99.5	8.3 σ
				Flat FB template			
HD	3D	U	Model I	867271.7	867060.1	423.2	19.1 σ
HD	2D A	U	Model I	867284.2	867122.9	322.5	16.5 σ
HD	2D B	U	Model I	867624.3	867464.0	320.7	16.4 σ
HD	2D C	U	Model I	867322.7	867158.2	329.0	16.6 σ
Interpolated	3D	U	Model I	867287.4	867081.2	412.4	18.9 σ
GALPROP	3D	U	Model I	868214.6	868040.9	347.6	17.2 σ

Detection significance

Template choices				Results			
Hadr. / Bremss.	IC	FB	Sgr dSph	$-\log(\mathscr{L}_{\text{Base}})$	$-\log(\mathscr{L}_{\text{Base+Sgr}})$	$\text{TS}_{\text{Source}}$	Significance
				Default model			
HD	3D	S	Model I	866680.6	866633.0	95.2	8.1 σ
				Alternative background templates			
HD	2D A	S	Model I	866847.1	866810.9	72.3	6.9 σ
HD	2D B	S	Model I	867234.9	867192.1	85.8	7.8 σ
HD	2D C	S	Model I	866909.4	866868.5	81.7	7.4 σ
Interpolated	3D	S	Model I	867595.4	867567.4	56.0	5.8 σ
GALPROP	3D	S	Model I	866690.5	866640.8	99.5	8.3 σ
				Flat FB template			
HD	3D	U	Model I	867271.7	867060.1	423.2	19.1 σ
HD	2D A	U	Model I	867284.2	867122.9	322.5	16.5 σ
HD	2D B	U	Model I	867624.3	867464.0	320.7	16.4 σ
HD	2D C	U	Model I	867322.7	867158.2	329.0	16.6 σ
Interpolated	3D	U	Model I	867287.4	867081.2	412.4	18.9 σ
GALPROP	3D	U	Model I	868214.6	868040.9	347.6	17.2 σ

Detection significance

Template choices				Results			
Hadr. / Bremss.	IC	FB	Sgr dSph	$-\log(\mathscr{L}_{\text{Base}})$	$-\log(\mathscr{L}_{\text{Base+Sgr}})$	$\text{TS}_{\text{Source}}$	Significance
				Default model			
HD	3D	S	Model I	866680.6	866633.0	95.2	8.1 σ
				Alternative background templates			
HD	2D A	S	Model I	866847.1	866810.9	72.3	6.9 σ
HD	2D B	S	Model I	867234.9	867192.1	85.8	7.8 σ
HD	2D C	S	Model I	866909.4	866868.5	81.7	7.4 σ
Interpolated	3D	S	Model I	867595.4	867567.4	56.0	5.8 σ
GALPROP	3D	S	Model I	866690.5	866640.8	99.5	8.3 σ
				Flat FB template			
HD	3D	U	Model I	867271.7	867060.1	423.2	19.1 σ
HD	2D A	U	Model I	867284.2	867122.9	322.5	16.5 σ
HD	2D B	U	Model I	867624.3	867464.0	320.7	16.4 σ
HD	2D C	U	Model I	867322.7	867158.2	329.0	16.6 σ
Interpolated	3D	U	Model I	867287.4	867081.2	412.4	18.9 σ
GALPROP	3D	U	Model I	868214.6	868040.9	347.6	17.2 σ

Detection significance

Template choices				Results			
Hadr. / Bremss.	IC	FB	Sgr dSph	$-\log(\mathscr{L}_{\text{Base}})$	$-\log(\mathscr{L}_{\text{Base+Sgr}})$	$\text{TS}_{\text{Source}}$	Significance
				Default model			
HD	3D	S	Model I	866680.6	866633.0	95.2	8.1 σ
				Alternative background templates			
HD	2D A	S	Model I	866847.1	866810.9	72.3	6.9 σ
HD	2D B	S	Model I	867234.9	867192.1	85.8	7.8 σ
HD	2D C	S	Model I	866909.4	866868.5	81.7	7.4 σ
Interpolated	3D	S	Model I	867595.4	867567.4	56.0	5.8 σ
GALPROP	3D	S	Model I	866690.5	866640.8	99.5	8.3 σ
				Flat FB template			
HD	3D	U	Model I	867271.7	867060.1	423.2	19.1 σ
HD	2D A	U	Model I	867284.2	867122.9	322.5	16.5 σ
HD	2D B	U	Model I	867624.3	867464.0	320.7	16.4 σ
HD	2D C	U	Model I	867322.7	867158.2	329.0	16.6 σ
Interpolated	3D	U	Model I	867287.4	867081.2	412.4	18.9 σ
GALPROP	3D	U	Model I	868214.6	868040.9	347.6	17.2 σ

What is the signal?

- No gas (lost to tidal and ram pressure stripping)
- Star formation ceased 2-3 Gyr ago
- ⇒*Not* hadronic emission (no CR hadrons from SF, no target hadrons)

The Galactic Plane as seen by *Fermi*

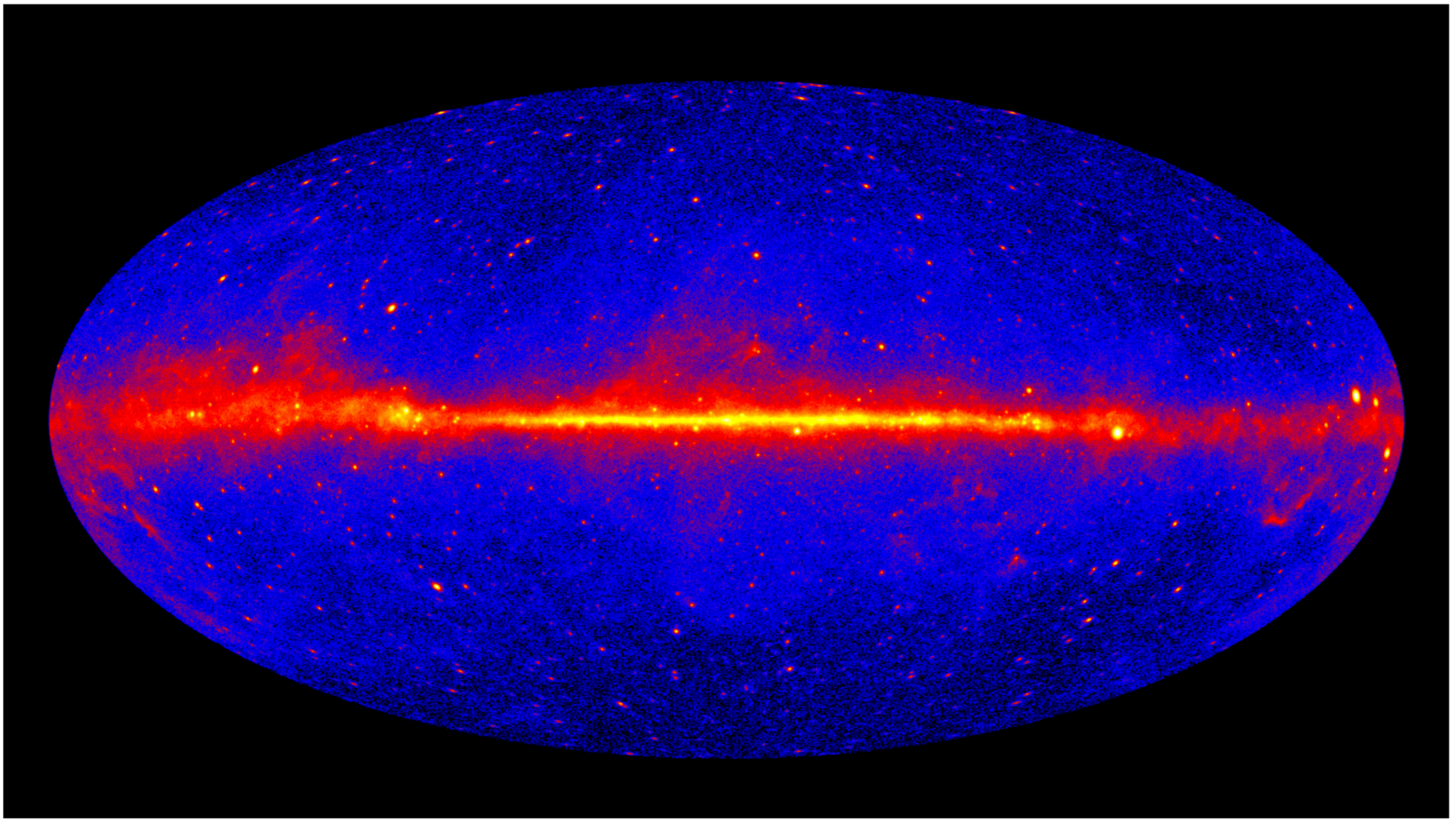

Figure 1: *Fermi*-LAT all sky image in Galactic co-ordinates. Credit: NASA/DoE.

What is the signal?

- No gas (lost to tidal and ram pressure stripping)
- Star formation ceased 2-3 Gyr ago
  - ⇒*Not* hadronic emission (no CR hadrons from SF, no target hadrons
- Signal traces stars (proviso: see below)
  - ⇒*Not* dark matter

What is the signal?

- Millisecond pulsars (MSPs)?
  - Pros:
    - MSPs generate ~GeV γ-ray signals amongst old stellar populations (e.g., globular clusters, 'GCE', M31…)
    - Signal expected to trace stars
- Cons:
  - At first sight, spectrum is wrong for MSPs

Spectrum

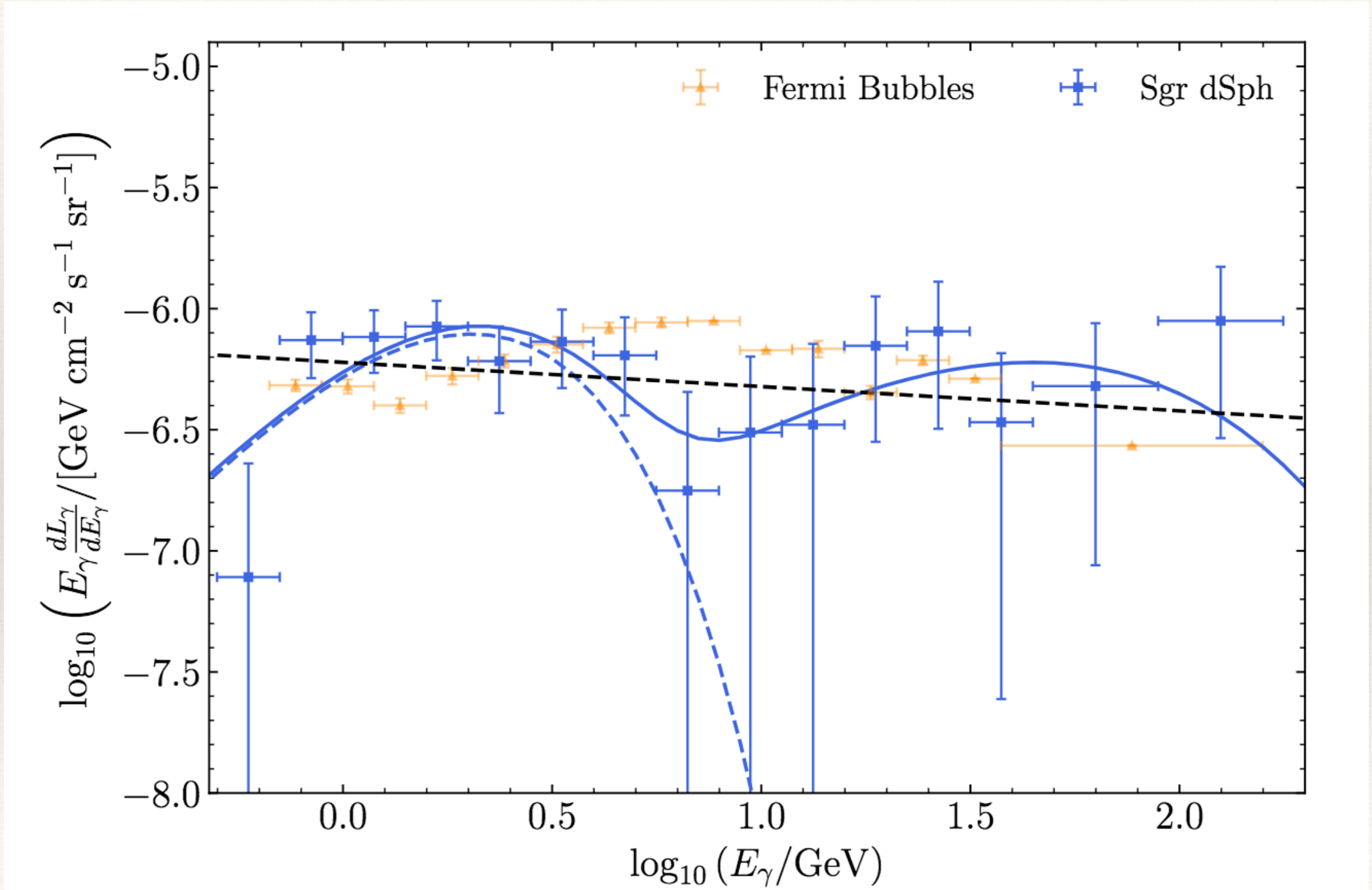
Fermi Bubbles
Sgr dSph
$\log_{10}\left(E_\gamma \frac{dL_\gamma}{dE_\gamma} / [\mathrm{GeV\ cm^{-2}\ s^{-1}\ sr^{-1}}]\right)$
$\log_{10}(E_\gamma/\mathrm{GeV})$
−5.0
−5.5
−6.0
−6.5
−7.0
−7.5
−8.0
0.0
0.5
1.0
1.5
2.0

What is the signal?

- Millisecond pulsars (MSPs)?
  - Pros:
    - MSPs generate ~GeV γ-ray signals amongst old stellar populations (e.g., globular clusters, 'GCE', M31…)
    - Signal expected to trace stars
  - Cons:
    - At first sight, spectrum is wrong for MSPs
    - γ-ray luminosity per stellar mass is much higher than for some other putatively MSP-dominated systems

γ-ray luminosity normalised to stellar mass

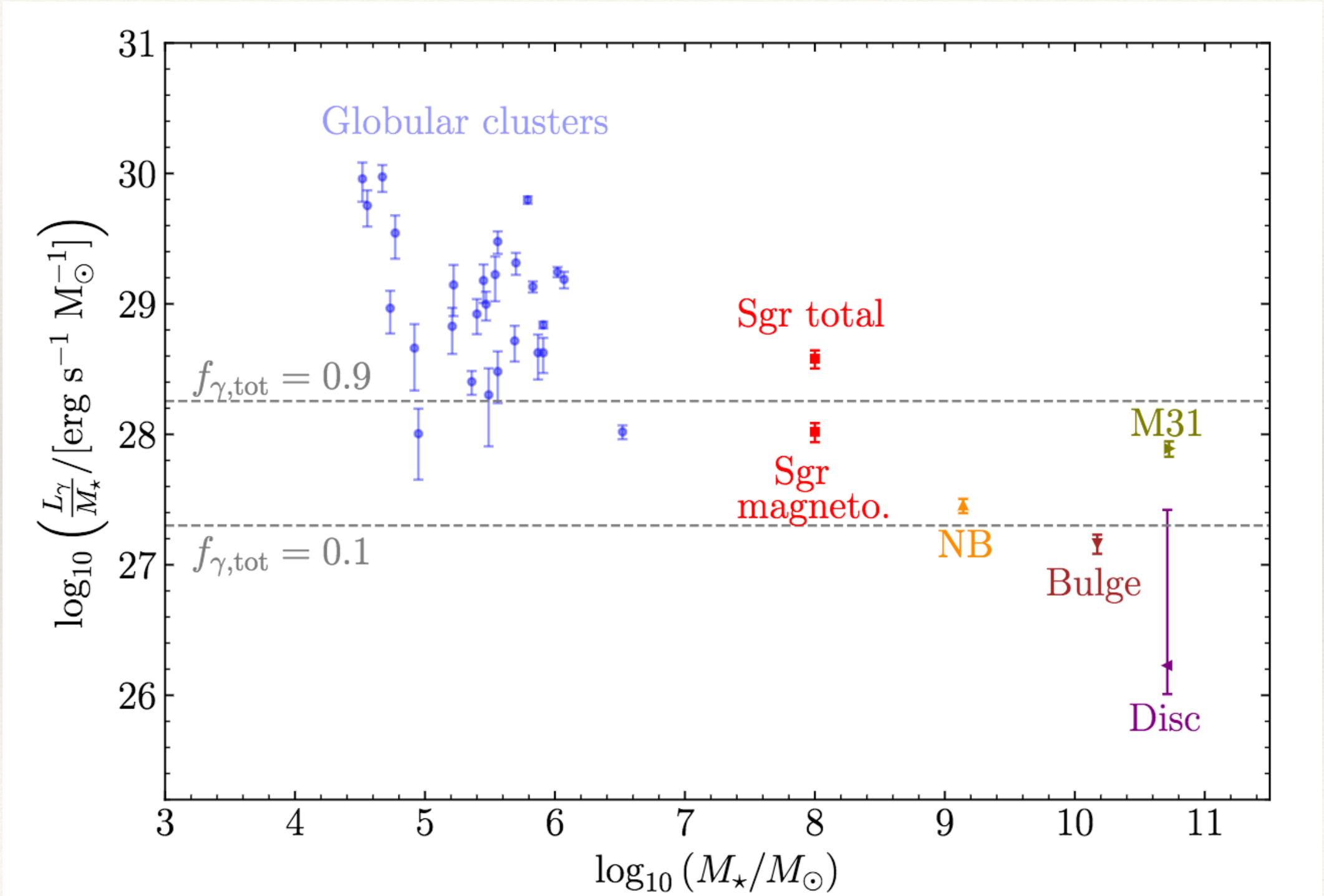

What is the signal?

- Unusual ISM conditions in Sgr dSph:
  - no gas
  - $\Rightarrow$ no way to anchor magnetic field lines
  - $\Rightarrow u_{ISRF} (= u_{CMB}) \gg u_B$
  - $\Rightarrow$ CR $e^{\pm}$ released into ISM *can only* radiate via Inverse Compton (negligible synchrotron in contrast to 'usual' situation for MSP pairs)

What is the signal?

- Physics of curvature radiation:
  - ~few GeV peak in SED of curvature radiation
    - ⇒ ~few TeV CR $e^{\pm}$
      - ⇒ ~few TeV CR $e^{\pm}$'s do ~100 GeV IC off CMB *as required*
- Can also self consistently relate the spectrum of the putative magnetospheric curvature radiation and the spectrum of the IC from the pairs released into the ISM

Spectrum: interpretation

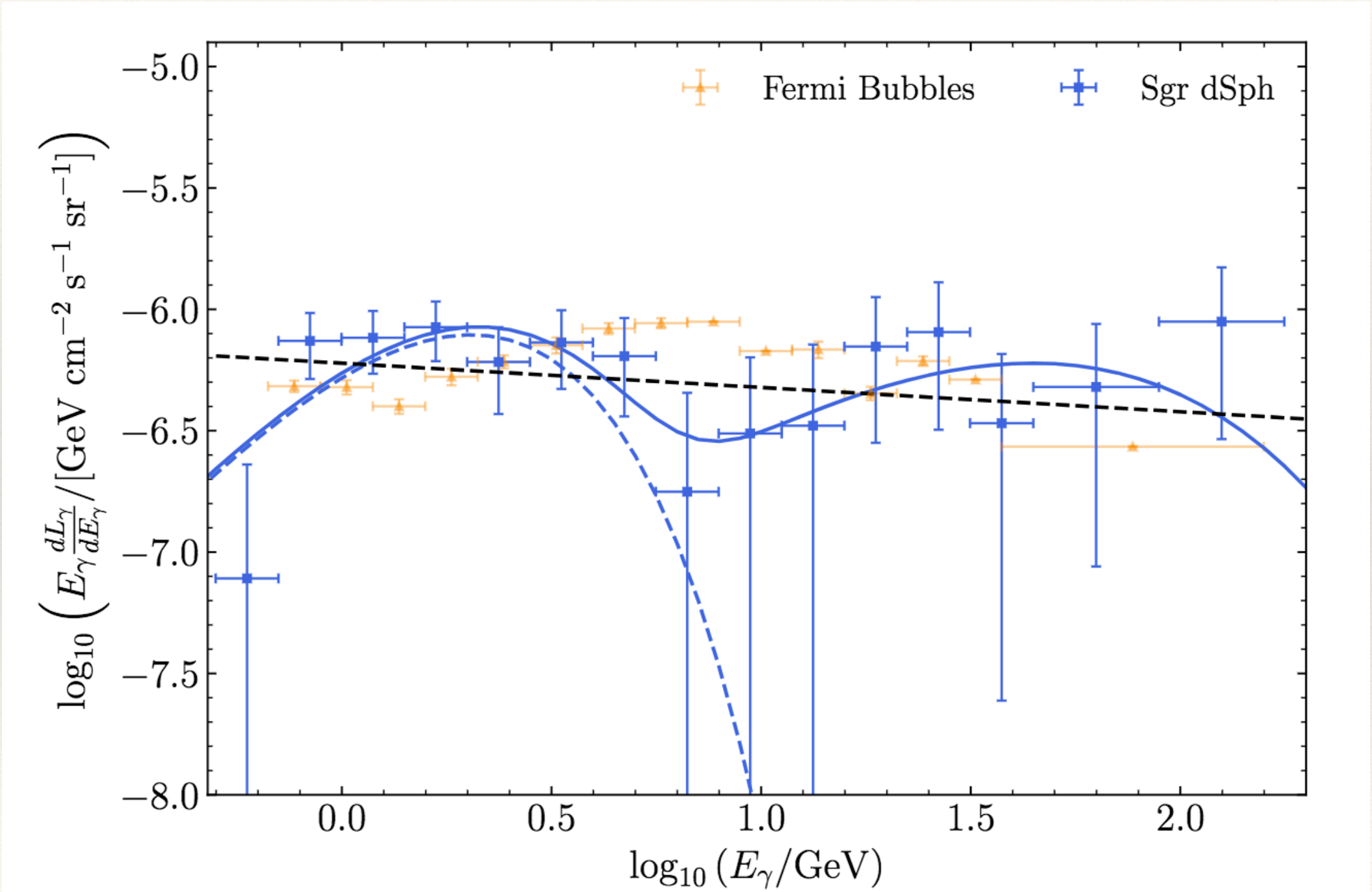

Spectrum: interpretation

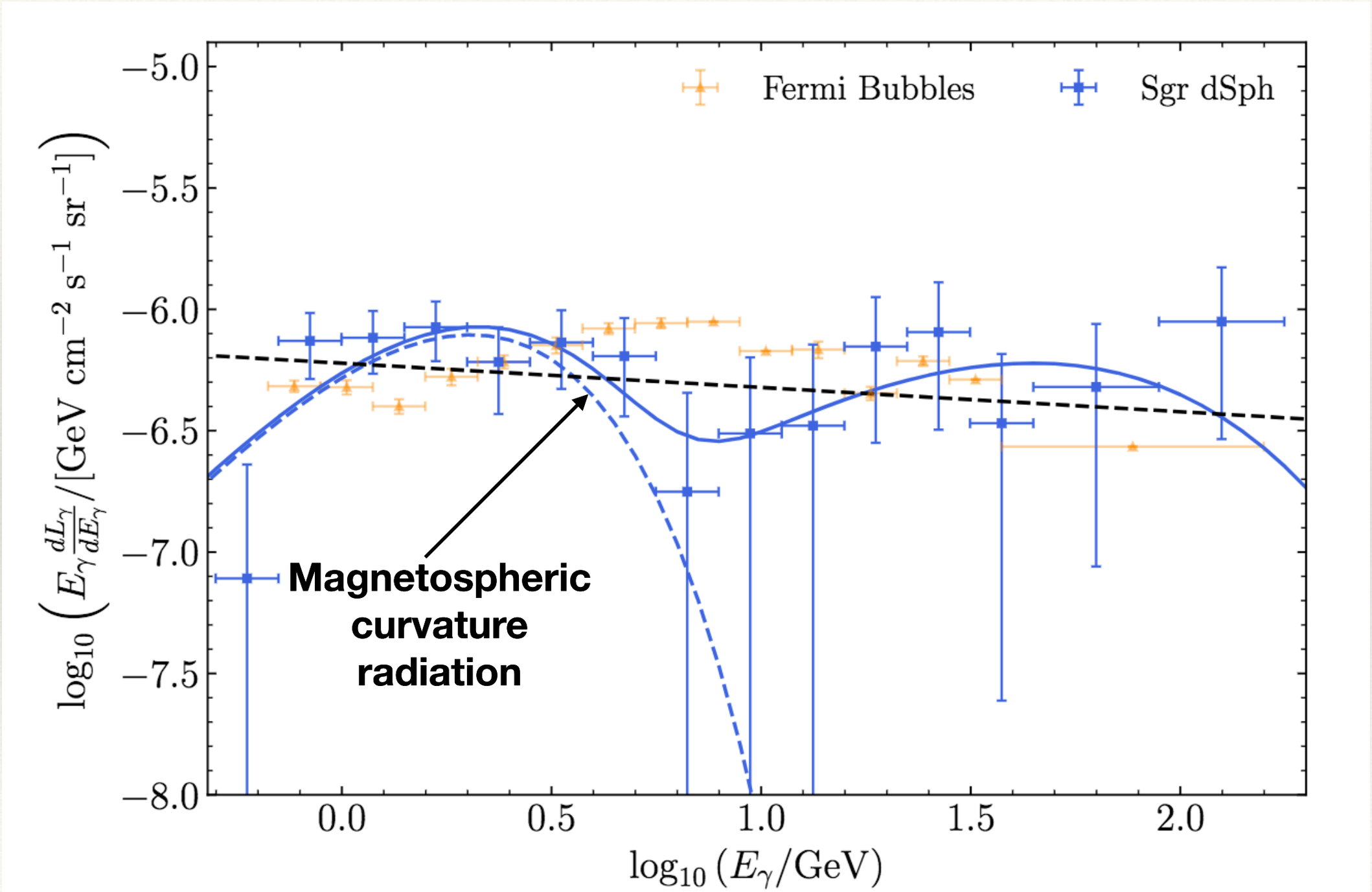

Spectrum: interpretation

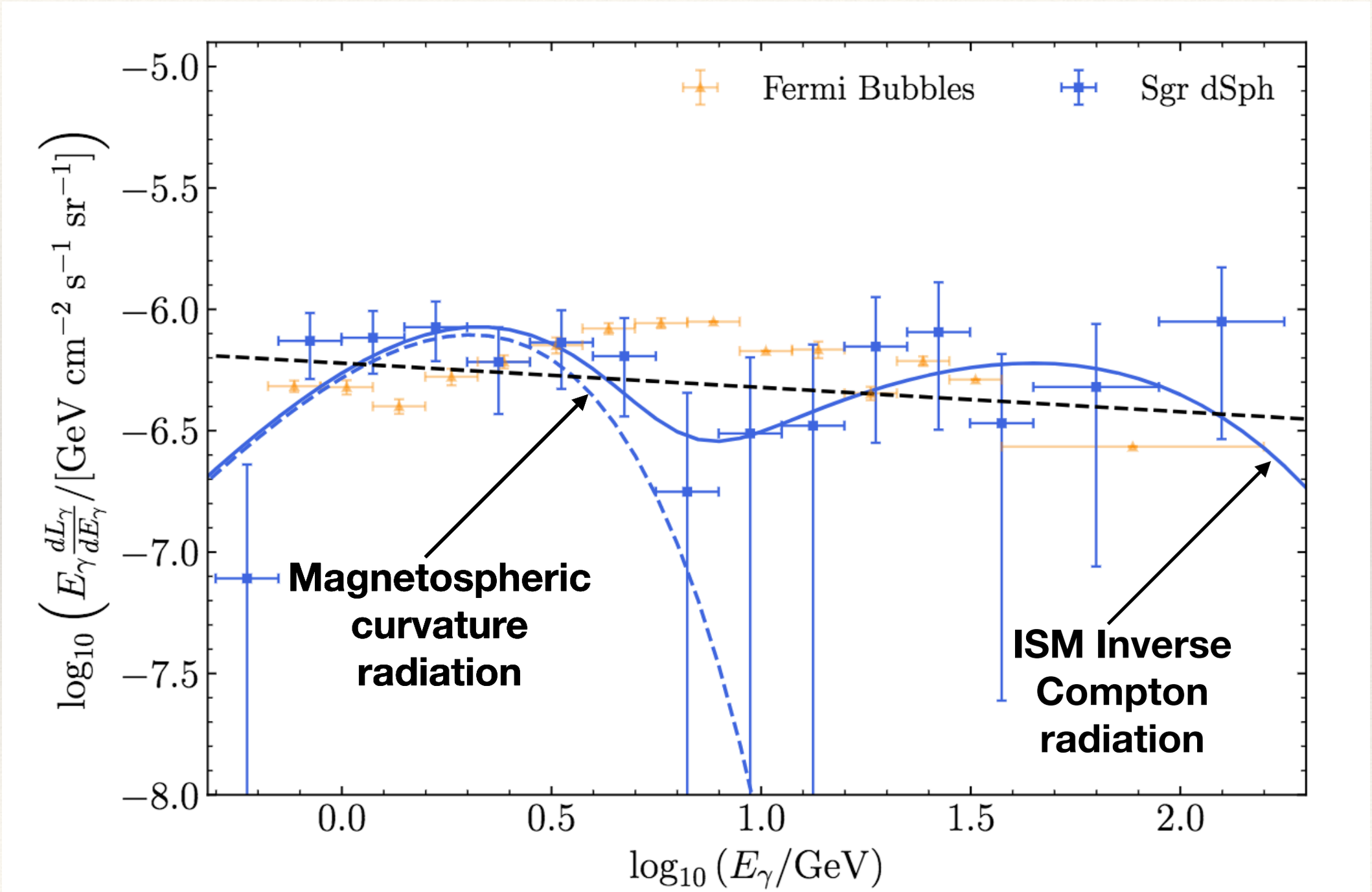

Spectrum: interpretation

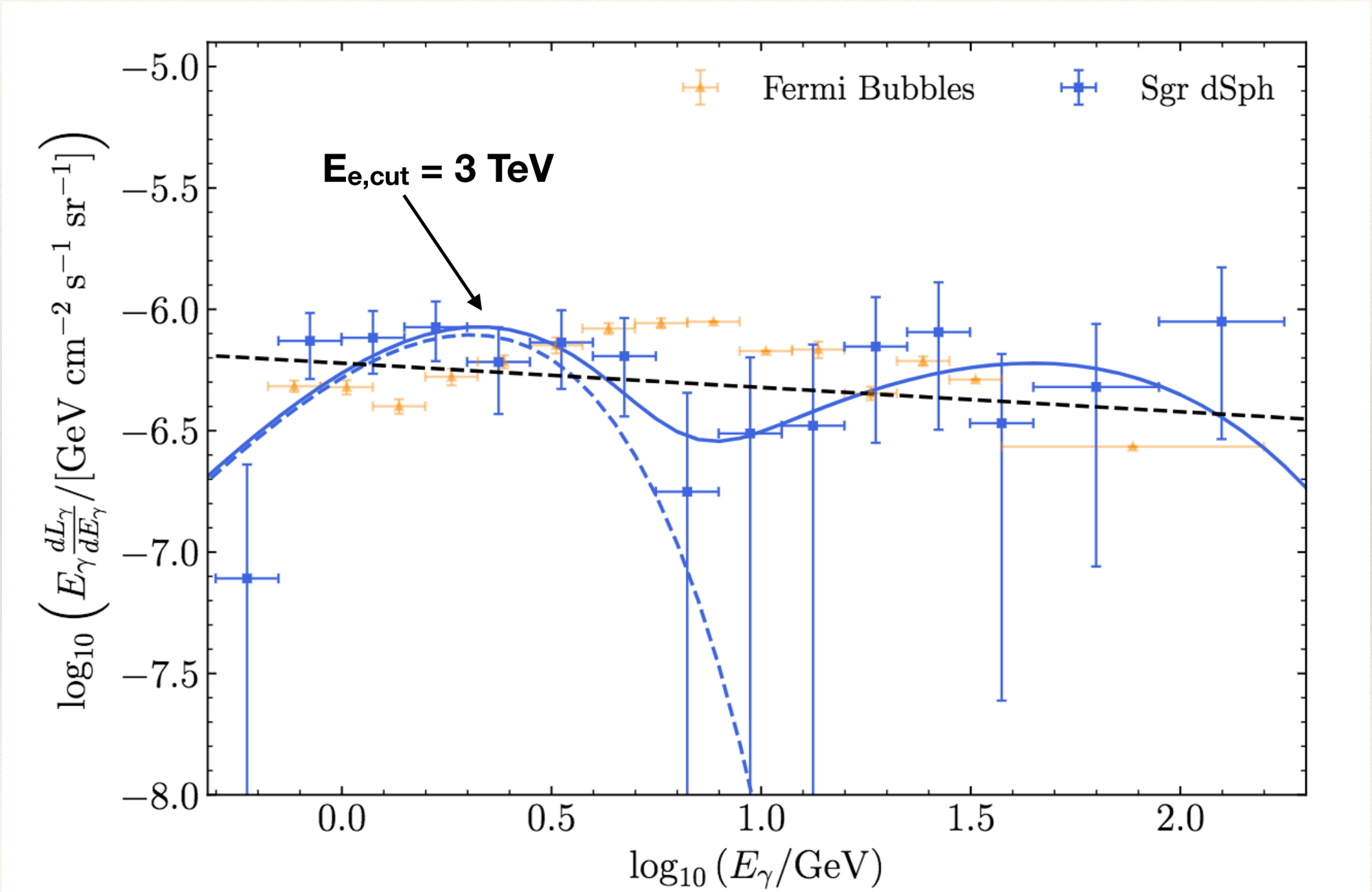

Spectrum: interpretation

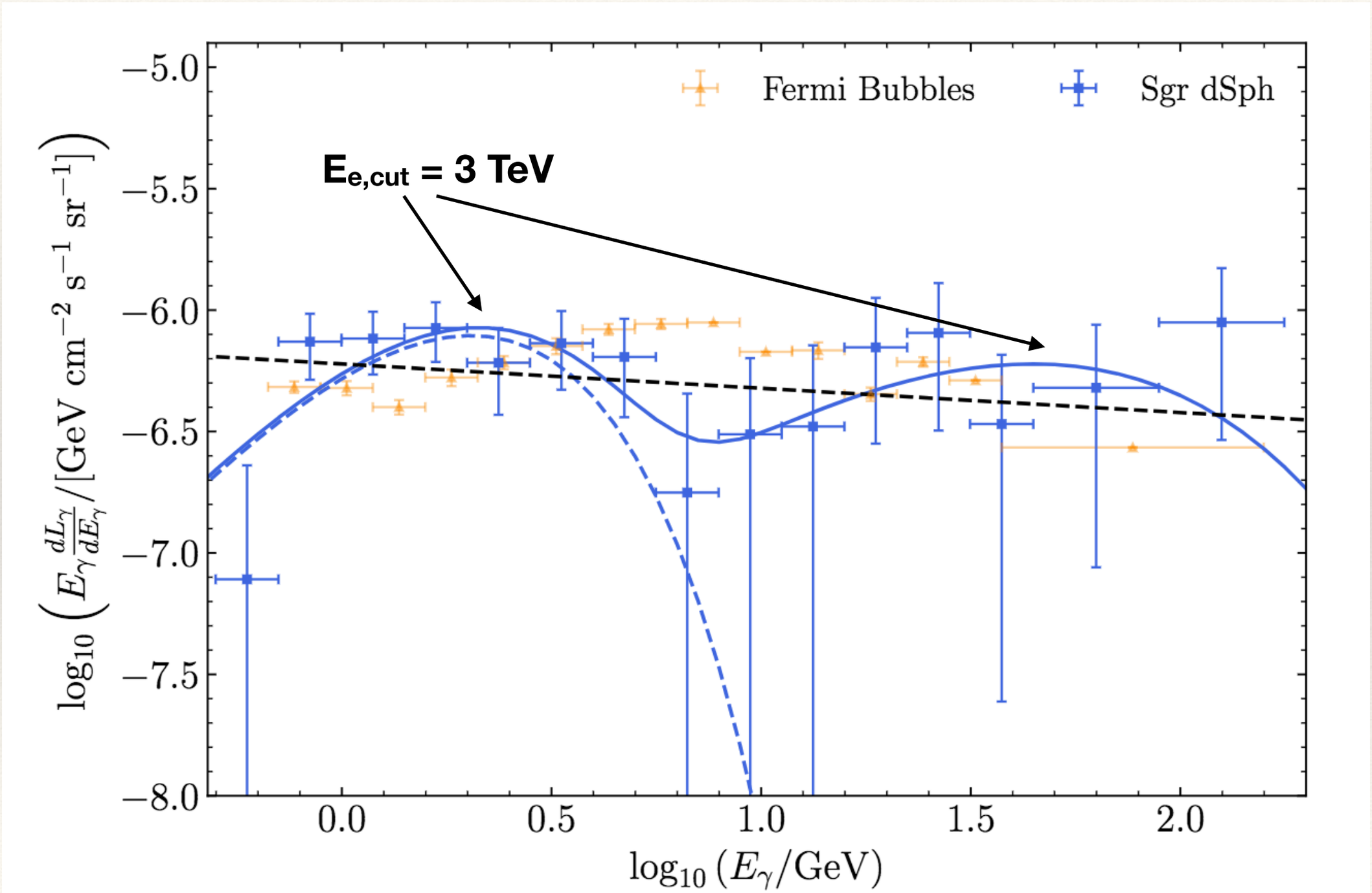

Spectrum: interpretation

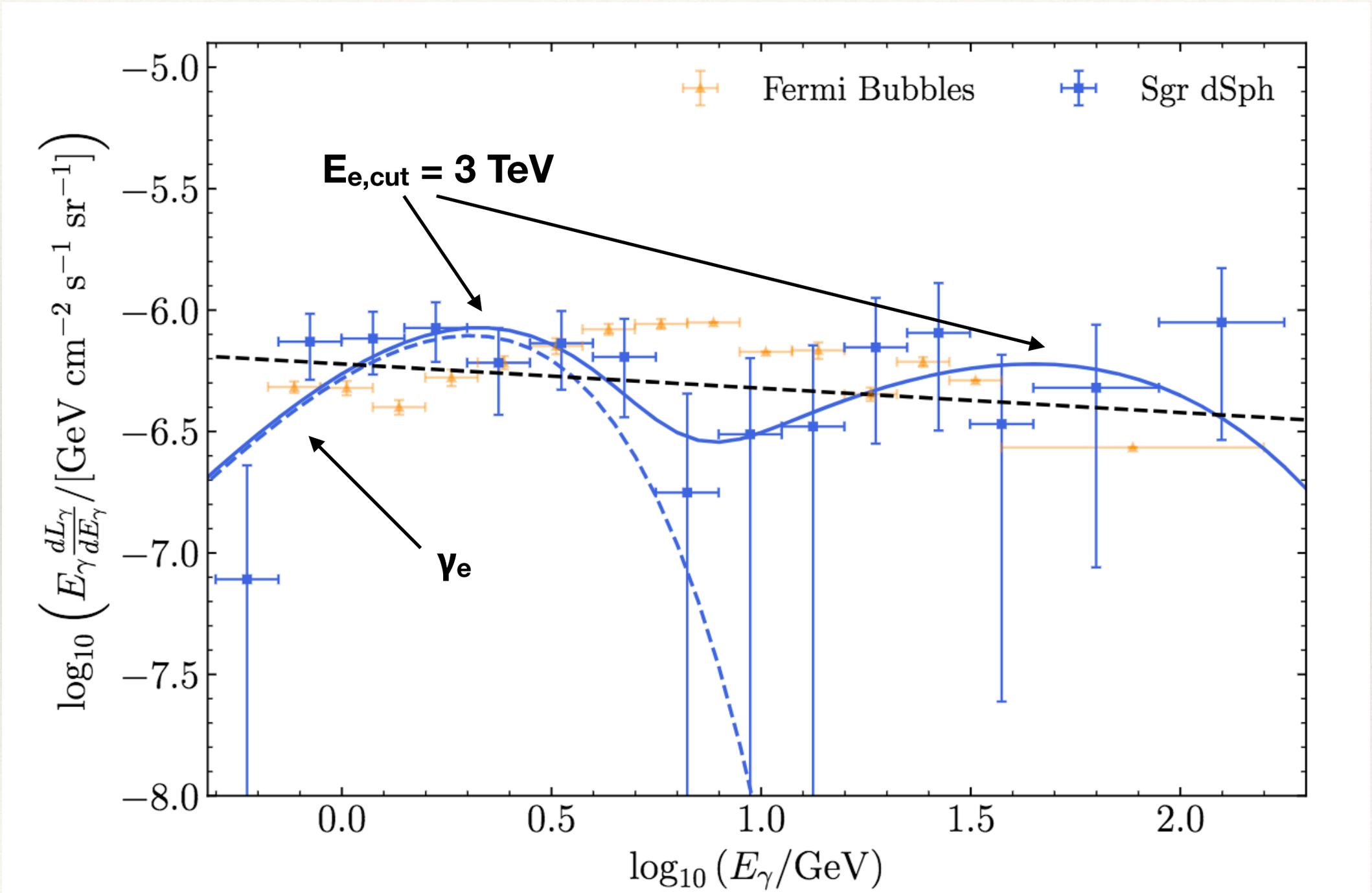

Spectrum: interpretation

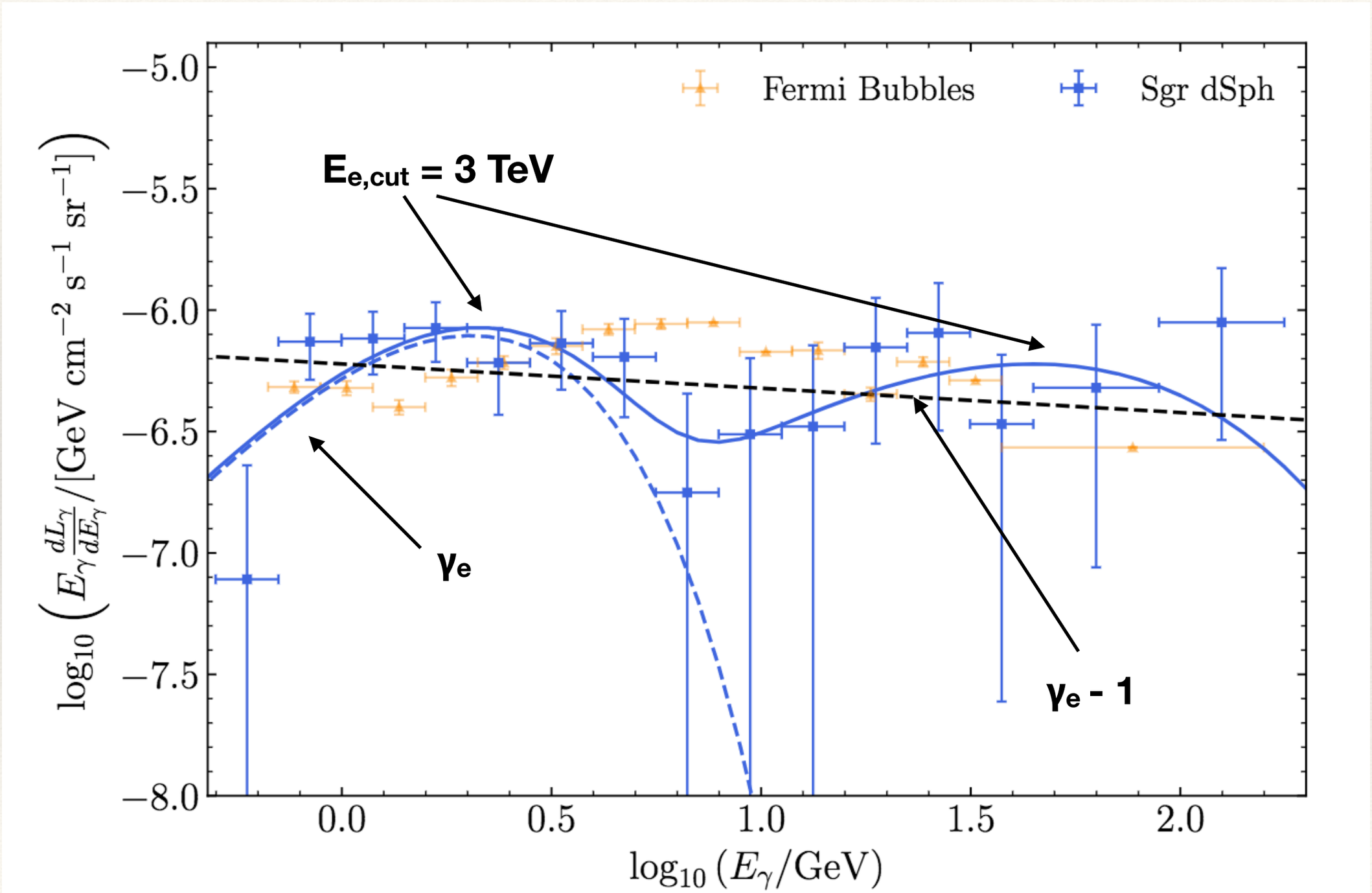

Spectrum: interpretation

- Overall spectrum consistent with same population of CR $e^{\pm}$ radiating in MSP magnetospheres
- …then leaking into ISM
- …then cooling/radiating via IC off CMB

Spectrum: interpretation

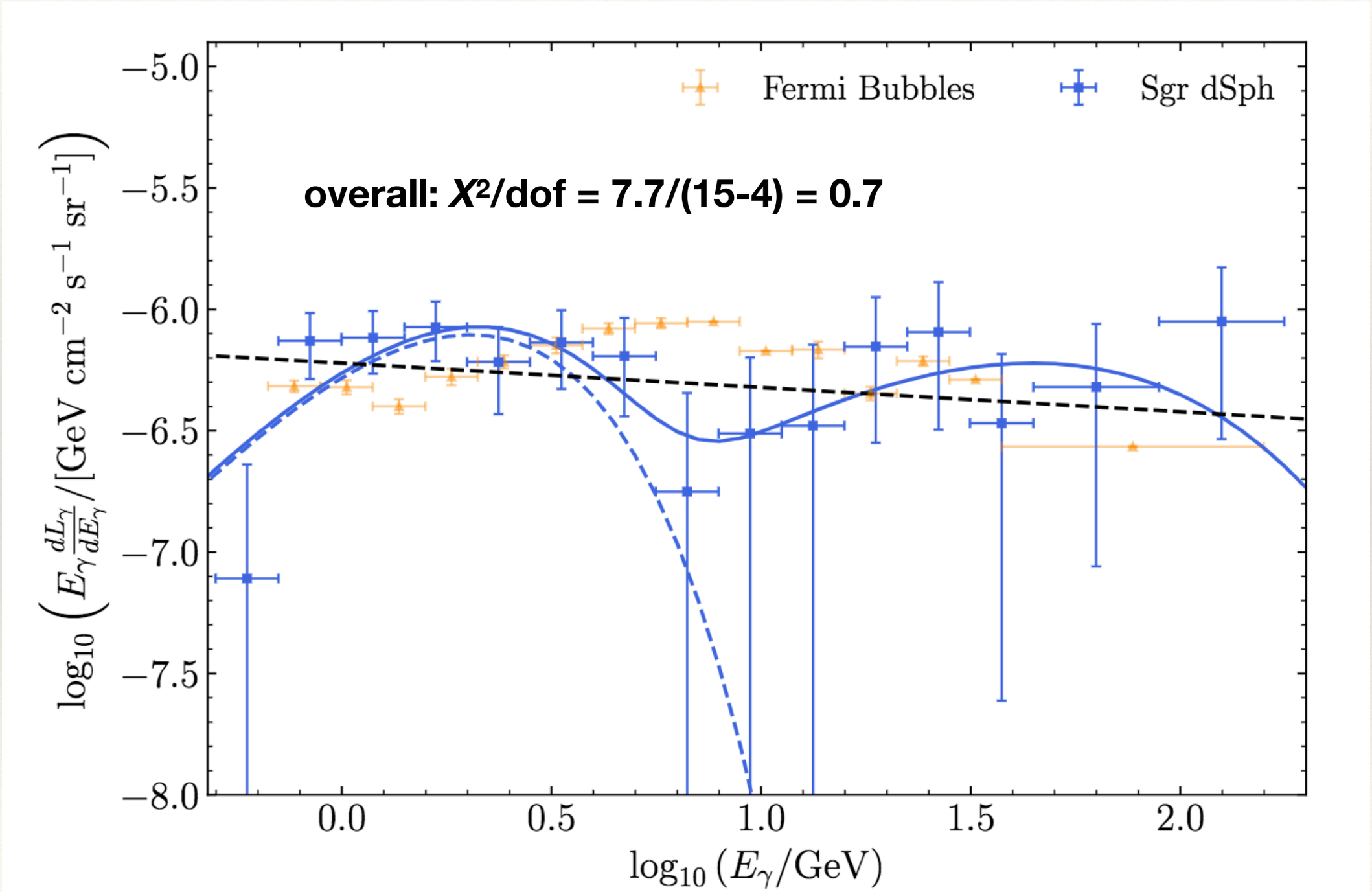

(Slight) displacement of signal

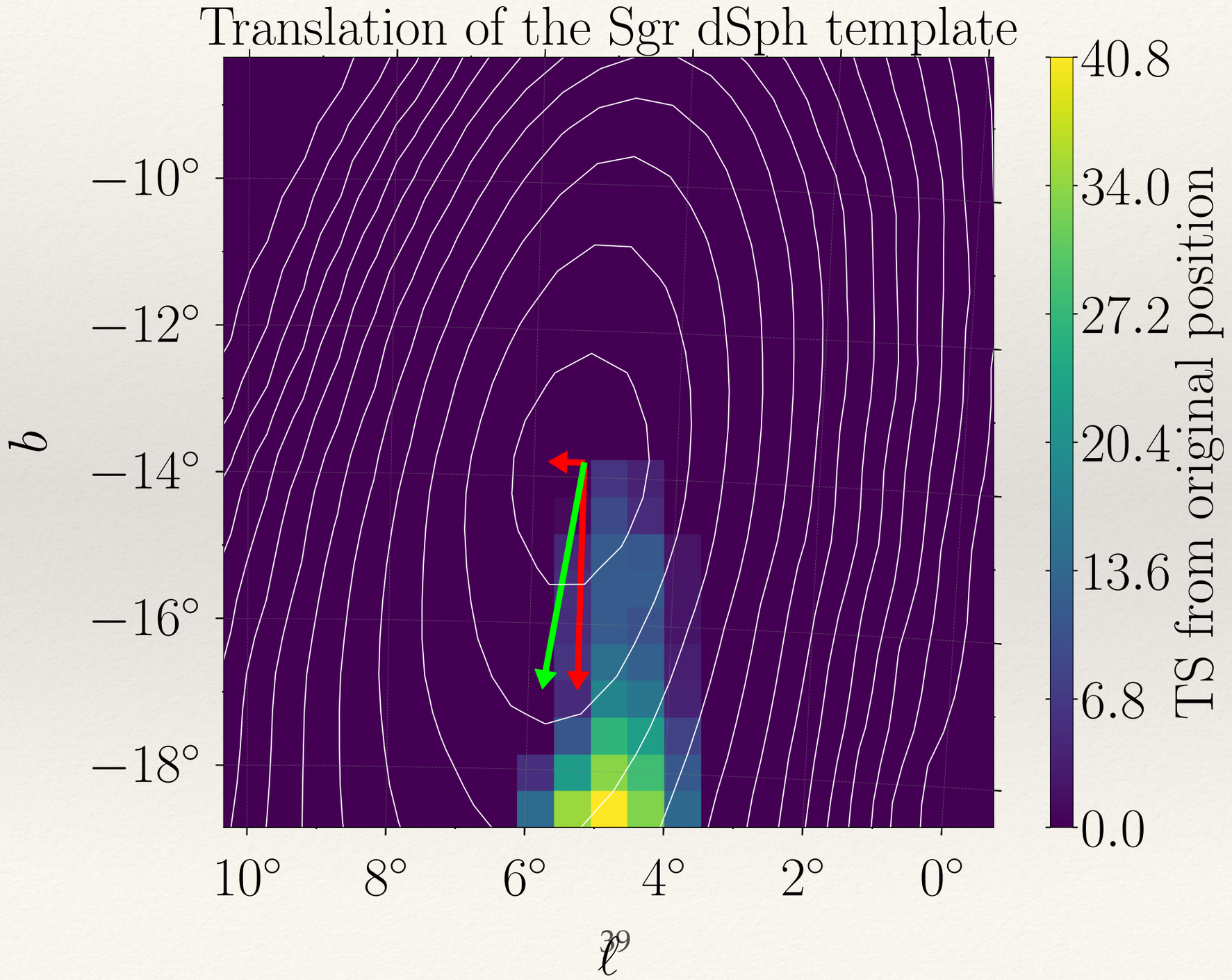

Implications

γ-ray luminosity normalised to stellar mass

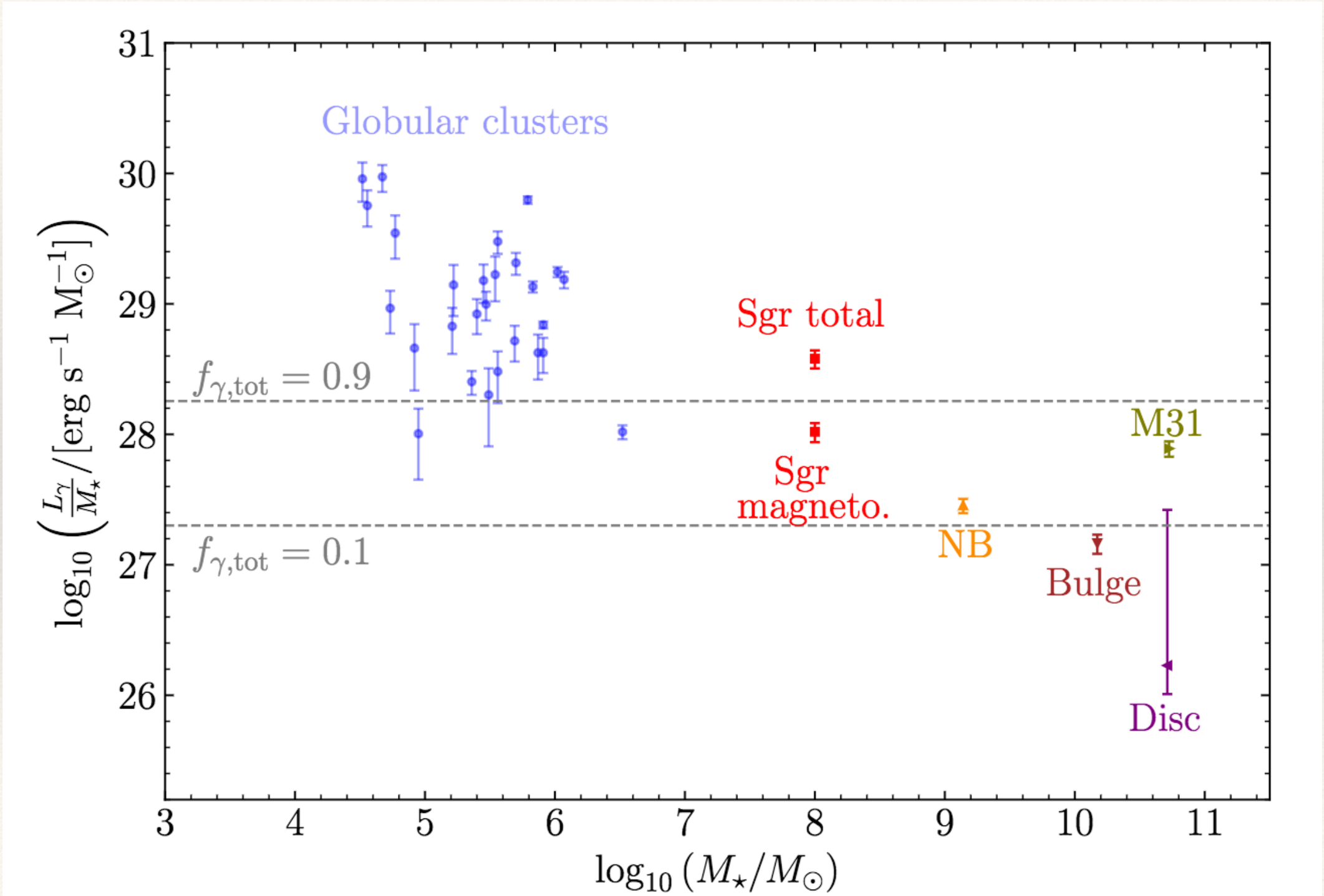

γ-ray luminosity normalised to stellar mass

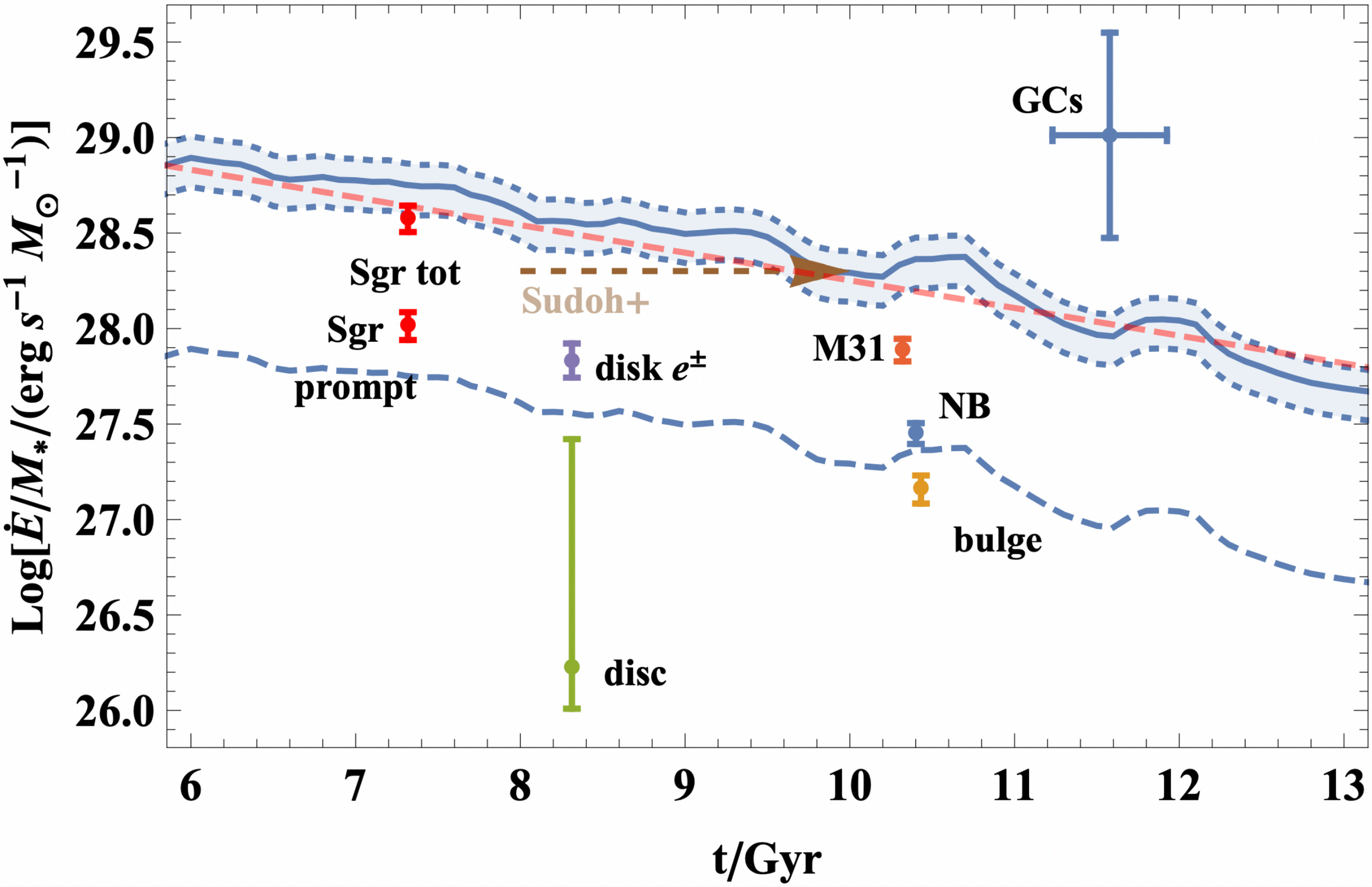

γ-ray luminosity normalised to stellar mass

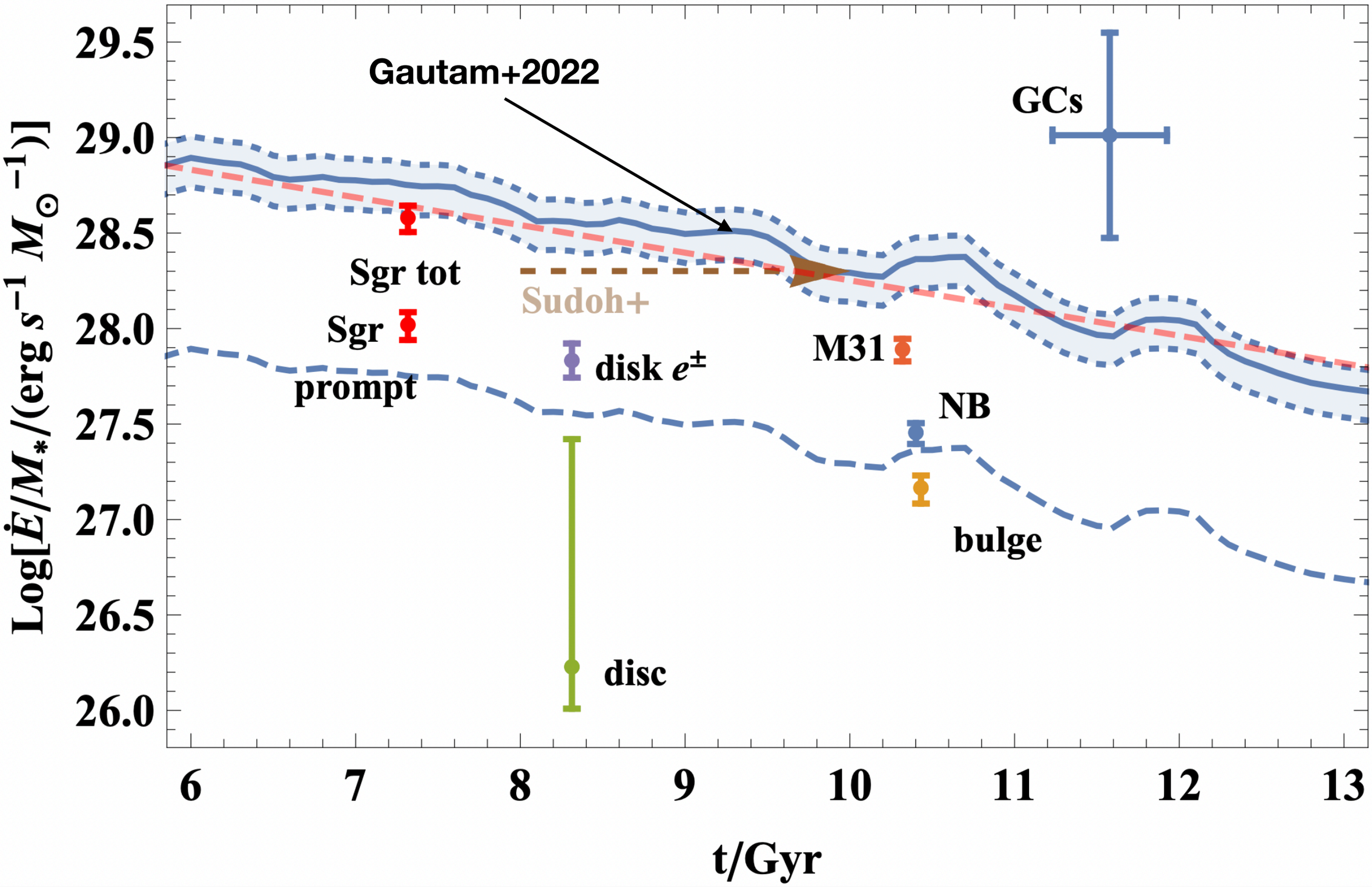

γ-ray luminosity normalised to stellar mass

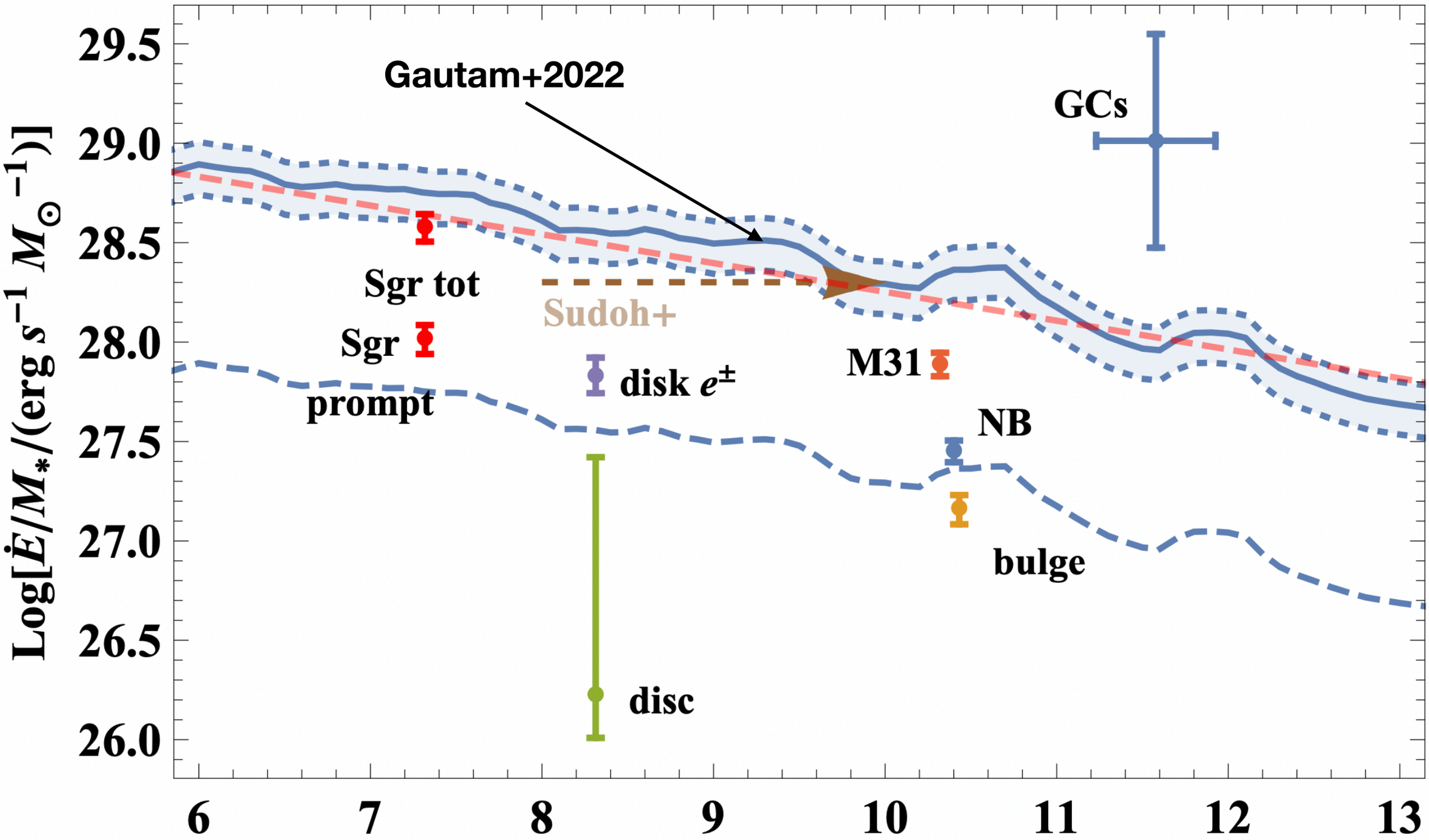

➡ The Sgr dSph is brighter than other systems because its stars are younger

γ-ray luminosity normalised to stellar mass

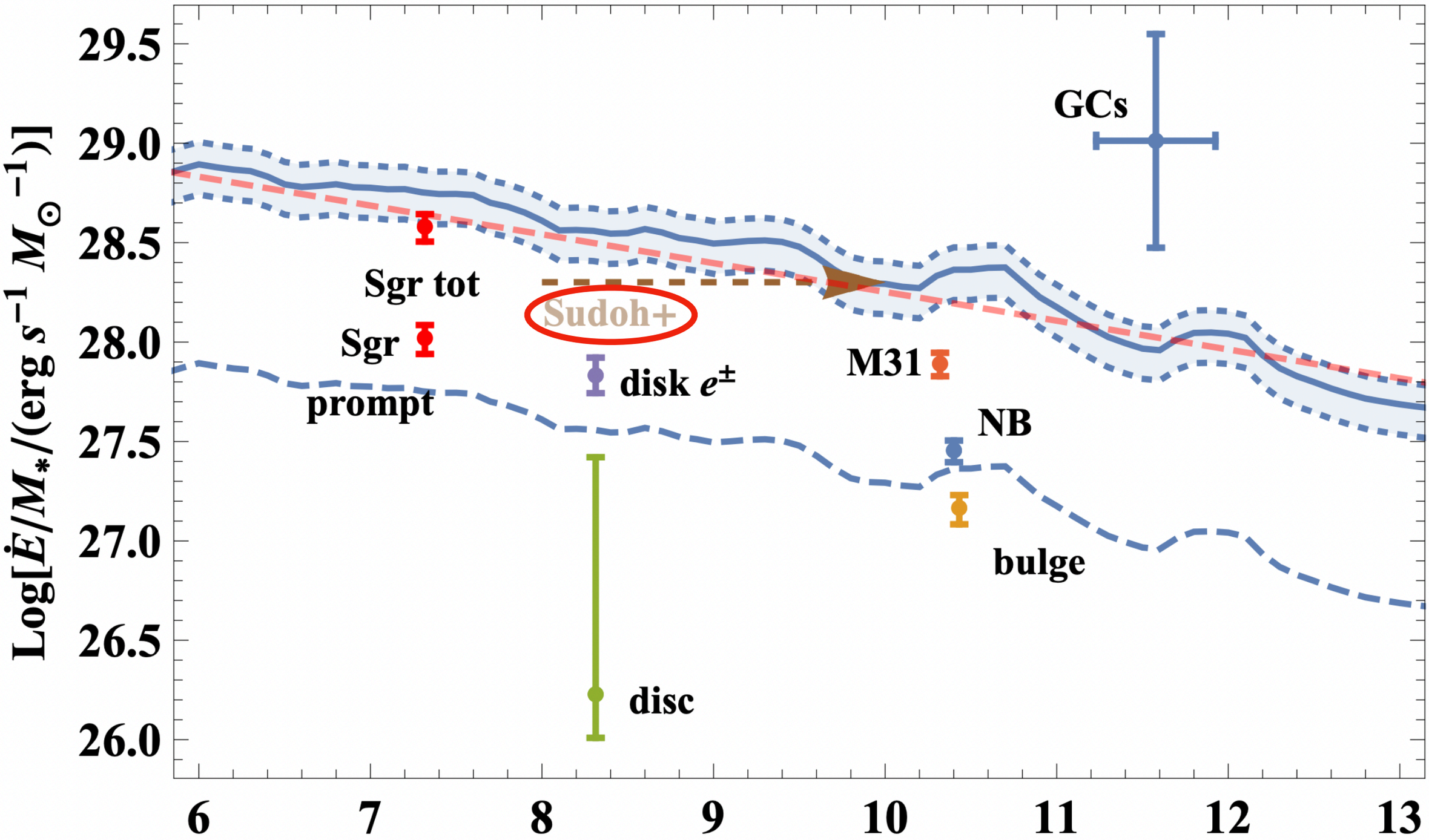

➡ The Sgr dSph is brighter than other systems because its stars are younger

γ-ray luminosity normalised to stellar mass

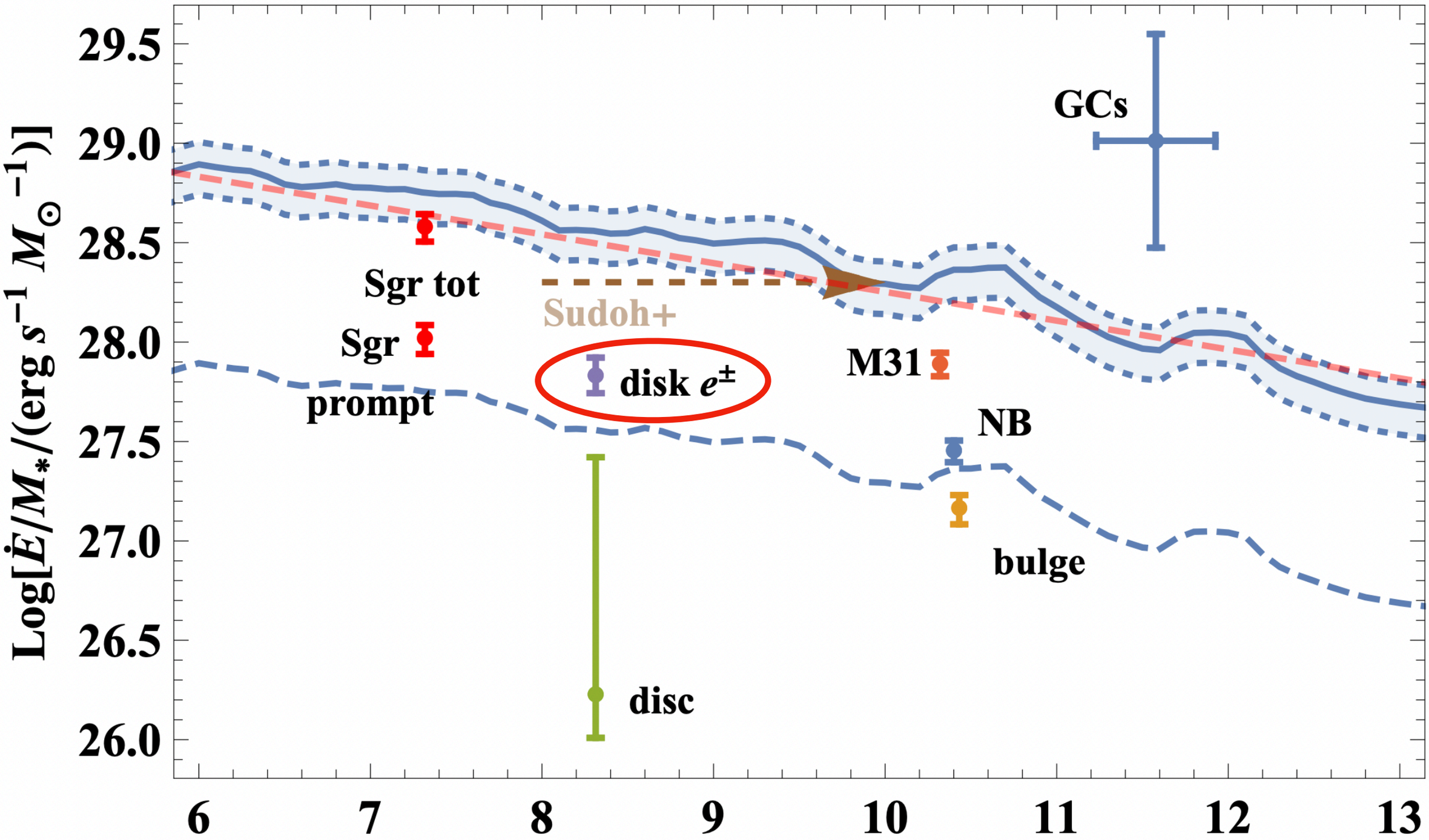

➡ The Sgr dSph is brighter than other systems because its stars are younger

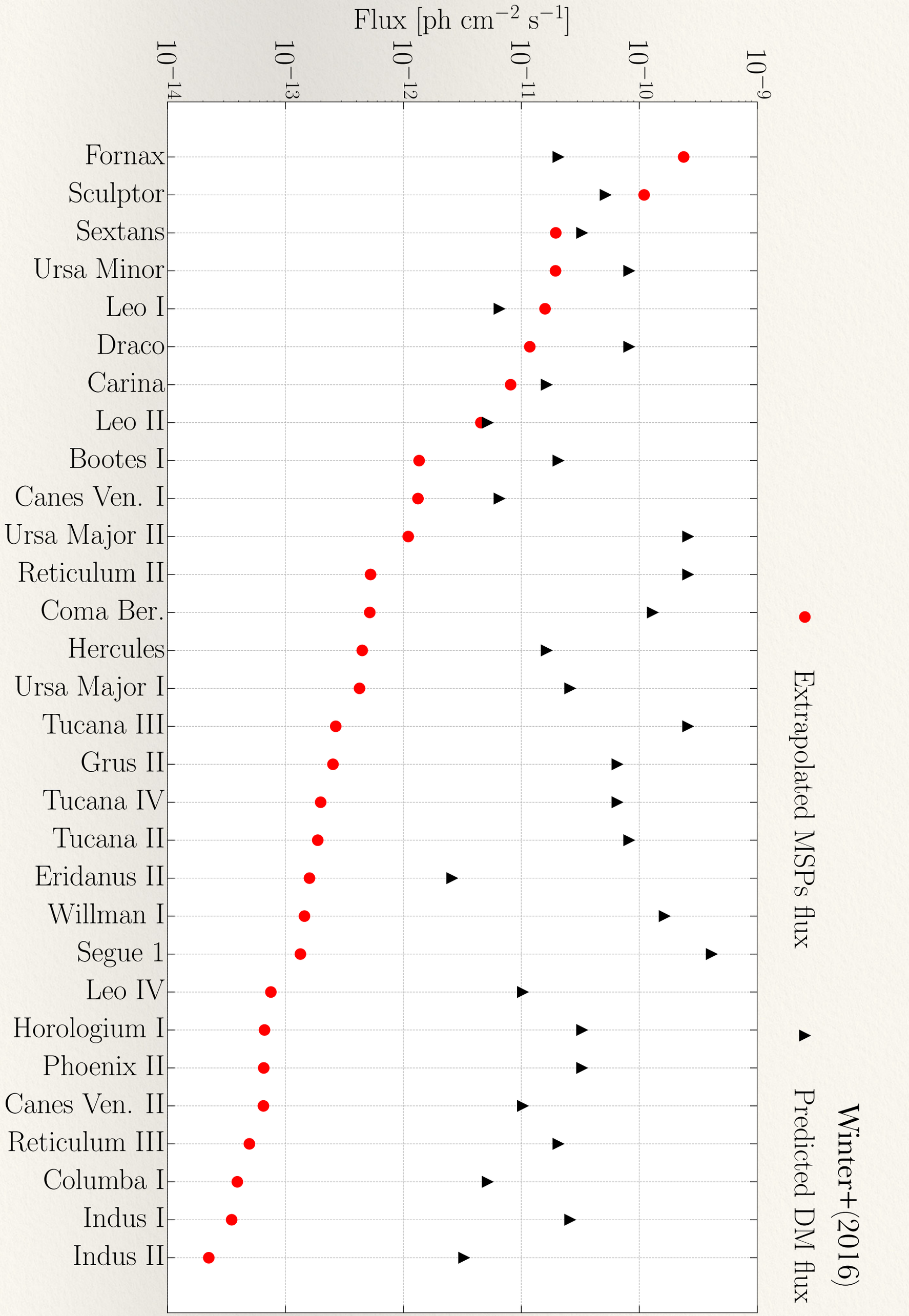
Flux [ph cm^{-2} s^{-1}]
10^{-14}
10^{-13}
10^{-12}
10^{-11}
10^{-10}
10^{-9}
Fornax
Sculptor
Sextans
Ursa Minor
Leo I
Draco
Carina
Leo II
Bootes I
Canes Ven. I
Ursa Major II
Reticulum II
Coma Ber.
Hercules
Ursa Major I
Tucana III
Grus II
Tucana IV
Tucana II
Eridanus II
Willman I
Segue 1
Leo IV
Horologium I
Phoenix II
Canes Ven. II
Reticulum III
Columba I
Indus I
Indus II
Extrapolated MSPs flux
Predicted DM flux
Winter+(2016)

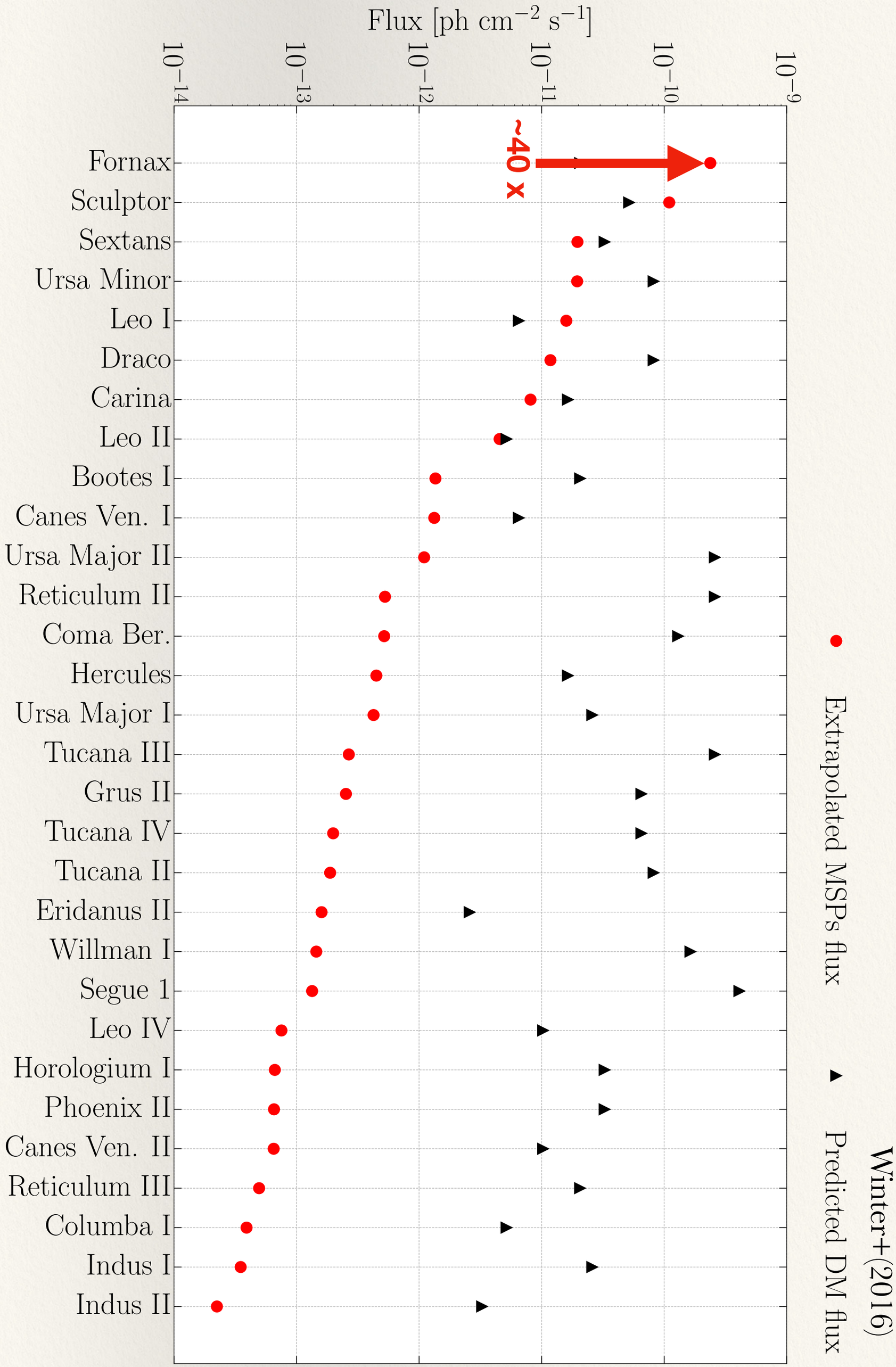
Flux [ph cm^{-2} s^{-1}]
10^{-14}
10^{-13}
10^{-12}
10^{-11}
10^{-10}
10^{-9}
~40 x
Fornax
Sculptor
Sextans
Ursa Minor
Leo I
Draco
Carina
Leo II
Bootes I
Canes Ven. I
Ursa Major II
Reticulum II
Coma Ber.
Hercules
Ursa Major I
Tucana III
Grus II
Tucana IV
Tucana II
Eridanus II
Willman I
Segue 1
Leo IV
Horologium I
Phoenix II
Canes Ven. II
Reticulum III
Columba I
Indus I
Indus II
Extrapolated MSPs flux
Predicted DM flux
Winter+(2016)

Flux [ph cm^{-2} s^{-1}]

10^{-14} 10^{-13} 10^{-12} 10^{-11} 10^{-10} 10^{-9}

~40 x

Fornax
Sculptor
Sextans
Ursa Minor
Leo I
Draco
Carina
Leo II
Bootes I
Canes Ven. I
Ursa Major II
Reticulum II
Coma Ber.
Hercules
Ursa Major I
Tucana III
Grus II
Tucana IV
Tucana II
Eridanus II
Willman I
Segue 1
Leo IV
Horologium I
Phoenix II
Canes Ven. II
Reticulum III
Columba I
Indus I
Indus II

Winter+(2016)

Predicted DM flux

Extrapolated MSPs flux

Implications

- Largely removes any residual motivation for the idea that Fermi Bubbles sub-structure be interpreted as γ-ray jets launched from the Galactic nucleus.
- WRT searches for the signatures of DM annihilation: astrophysical backgrounds in dwarf spheroidal galaxies can be stronger than previously appreciated. In general, a salutary example of how MSPs are a problem for indirect WIMP detection (cf. GCE).
- Our study lends support to the argument that MSPs contribute significantly to the energy budget of CR $e^{\pm}$ in galaxies with low specific star-formation rates.

Take-away messages

- We have detected ~1-100 GeV γ-ray emission from the Sagittarius dwarf spheroidal, the third-most massive satellite of the Milky Way (after LMC and SMC)
- The signal seems to be explained by millisecond pulsars belonging to the dwarf
- This discovery casts new light on MSPs as sources of non-thermal radiation and particles